https://doi.org/10.59761/RCR5148

Adsorption-induced segregation as a way to control the catalytic performance of palladium-based bimetallic catalysts

Andrey V. Bukhtiyarov,[a] Maxim A. Panafidin,[a] Igor P. Prosvirin,[a] Yan V. Zubavichus,[a] Alexander Yu. Stakheev,[b] Igor S. Mashkovsky,[b] Valerii I. Bukhtiyarov [a]

[a] *G.K.Boreskov Institute of Catalysis, Siberian Branch of the Russian Academy of Sciences, 630090 Novosibirsk, Russia*
[b] *N.D.Zelinsky Institute of Organic Chemistry of the Russian Academy of Sciences, 119991 Moscow, Russia*

The review analyzes recent publications devoted to the experimental and computational studies of adsorption-induced segregation effects in palladium-based bimetallic catalysts. The segregation processes are considered for two types of systems, those based on substitutional solid solutions (alloys) and on intermetallic compounds. The applicability of adsorption-induced segregation effects for fine tuning of active sites on the catalytic surface is discussed. The possibility of controlling catalytic properties in various reactions using these effects is analyzed. The prospects for the development of this research area are given in the conclusion.
The bibliography includes 138 references.
Keywords: adsorption-induced segregation, palladium, bimetallic catalyst, intermetallic compound, substitutional solid solution.

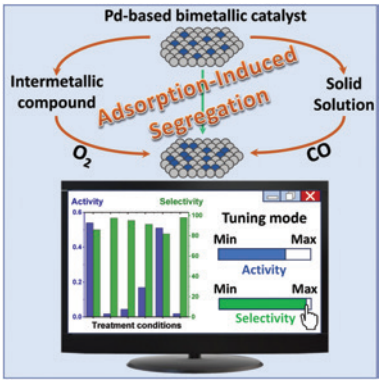

Contents

1. Introduction

Supported metal catalysts, which comprise metal nanoparticles deposited on various supports (Al_2O_3, SiO_2, zeolites, carbon materials, *etc*.), are widely used in chemical, petrochemical, and oil refining industries. The key characteristics that should be varied to attain the optimal catalytic performance include choice of the support (metal–support interaction), particle size and structure, and particle distribution over the surface. Along with the above characteristics, the introduction of a second metallic

A.V.Bukhtiyarov. Doctor of Chemistry, Researcher at the Department of Physicochemical Research at the Atomic and Molecular Level of BIC SB RAS.
E-mail: avb@catalysis.ru
M.A.Panafidin. Candidate of Sciences in Chemistry, Researcher at the Department of Physicochemical Research at the Atomic and Molecular Level, BIC SB RAS.
E-mail: mpanafidin@catalysis.ru
I.P.Prosvirin. Candidate of Sciences in Chemistry, Senior Researcher at the Department of Physicochemical Research at the Atomic and Molecular Level, BIC SB RAS.
E-mail: prosvirin@catalysis.ru
Y.V.Zubavichus. Doctor of Physics and Mathematics, Chief Researcher at the Department of Physicochemical Research at the Atomic and Molecular Level, BIC SB RAS.
E-mail: yvz@catalysis.ru
A.Yu.Stakheev. Doctor of Chemistry, Professor, Head of the Laboratory of Catalysis by Absorbed Metals and Metal Oxides, ZIOC RAS.
E-mail: st@ioc.ac.ru
I.S.Mashkovsky. Candidate of Sciences in Chemistry, Senior Researcher at the Laboratory of Catalysis by Supported Metals and Metal Oxides, ZIOC RAS.
E-mail: im@ioc.ac.ru
V.I. Bukhtiyarov. Doctor of Chemistry, Academician of RAS, Director of BIC SB RAS.
E-mail: vib@catalysis.ru
Current research interests of the authors: heterogeneous catalysis, selective hydrogenation, bimetallic catalysts, alloy catalysts, adsorption-induced segregation.

Translation: Yu.A.Pozdnyakova.

Received 1 August 2024

component into the catalyst is one of the main and most effective ways to control the catalytic performance of the supported systems. Therefore, bimetallic nanosystems attract considerable attention of researchers, first of all, in the field of heterogeneous catalysis.[1–11] This is due to the fact that these systems often exhibit a higher catalytic activity, selectivity, and stability compared to monometallic analogues in quite a few important industrial chemical processes such as the synthesis of vinyl acetate,[12] low-temperature CO oxidation,[13–15] catalytic NO reduction,[16,17] direct synthesis of hydrogen peroxide,[18] selective hydrogenation of acetylene (phenylacetylene) to ethylene (styrene),[19,20] selective oxidation of alcohols,[21] *etc*. Higher catalytic performance of a bimetallic system compared to the sum of the catalytic performances of the monometallic components is referred to as the synergistic effect.[6] The activity and selectivity of bimetallic catalysts are often discussed in terms of the so-called concepts of ensemble effect (geometric factors) and ligand effect (electronic factors).[14,22–26] The former implies the formation of certain surface structures on the domains of one metal (metal A) upon dilution by atoms of the second metal (metal B). The latter effect implies charge transfer between atoms A and B or change in the hybridization of atomic orbitals involving one or both metals *via* the formation of heteronuclear metal–metal bonds. Most studies currently available from the literature are devoted to the ensemble effect. As a rule, they imply that catalytic chemical reactions are accompanied by cleavage of chemical bonds to give molecules adsorbed on bimetallic alloy nanoparticles. These processes are mainly determined by the surface composition of the particles and, hence, the exact geometry of the polymetallic sites on the surface.

Despite numerous studies devoted to synergistic effects associated with the use of bimetallic catalysts, the mutual influence of components can hardly be generalized, because it may be considerably different for various catalytic systems. Nevertheless, most researchers agree that investigation of the composition of the sample surface is the key to understanding the role of the second component in bimetallic catalysts, since the component ratio on the alloy surface may considerably differ from the bulk composition of nanoparticles.[1,2,5–9,27,28] This is due to the fact that the chemical composition and structure of the active sites in bimetallic systems are determined by not only the ratio of the metals specified at the catalyst synthesis. The surface structure can markedly change both under the action of the reaction medium, *i.e*., directly during the catalytic reaction,[3,4,29] and upon particular types of catalyst pretreatment with various gases.[30–33] It is noteworthy that segregation effects related to the enrichment of the nanoparticle surface with one of the components upon adsorption of small molecules from a gas medium or during the catalytic reaction attract increasing attention of researchers specializing in this field. For example, factors determining the surface composition of bimetallic catalysts during adsorption of various gases were analyzed in detail by Nørskov and co-workers[34] and in a review of Zafeiratos *et al*.[35] It was shown[36] that the adsorption-induced segregation can also considerably change the surface composition of core–shell nanoparticles. Although there are quite a few publications addressing the segregation, the deliberate use of this phenomenon to fine-tune the surface composition and morphology and, hence, to generate various types of active sites in bimetallic catalysts has not received adequate attention. Meanwhile, this approach has a considerable potential for practical applications. In particular, the adsorption-induced segregation can be used to control the composition of the outer surface of the Pd-based bimetallic particles in order to optimize the properties of selective hydrogenation catalysts. This possibility was demonstrated by Anderson and co-workers,[37,38] who established experimentally that the catalyst activity and selectivity in the triple C≡C bond hydrogenation to the double C=C bond can be tuned *via* adsorption of CO. Only in recent years, researchers began to be interested in using this approach to control the catalytic properties of bimetallic systems. For example, a quite recent review by Stakheev and co-workers,[39] devoted to single-site and single-atom alloy systems, includes a small part addressing fine tuning of the active site structure by adsorption-induced segregation. However, the possibility of using adsorption-induced segregation in catalysis and the growing interest in this area are only briefly indicated in the review.

It is noteworthy that the nature of segregation processes can differ considerably depending on the type of bimetallic system. Therefore, this review addresses palladium-based bimetallic systems in order to analyze the differences between these processes in substitutional solid solutions (PdAu, PdAg, PdCu, *etc*.) and intermetallic compounds (PdIn, PdGa, PdZn, *etc*.).

For example, in the case of PdAg and PdAu bimetallic systems, which form a continuous series of substitutional solid solutions[40–42] that are not prone to structural ordering, treatment with CO in a definite temperature range results in the surface enrichment with palladium to give single-atom sites and Pd_n polynuclear surface clusters. Meanwhile, in the case of intermetallics such as PdIn or PdGa, the segregation caused by CO adsorption is manifested to a minor extent.[42–44] However, the oxidative treatment with oxygen at elevated temperature induces predominant oxidation of the component that has higher oxygen affinity, that is, indium (or gallium). This enables controlled generation of surface structures with neighbouring metal (Pd) and metal oxide domains and also $Pd@M_2O_3$ core–shell structures (where M = In or Ga).

This review presents literature data dealing with bimetallic systems based on palladium, since particularly these systems have been studied most actively in recent years regarding the adsorption-induced segregation effect. A brief account is given of different types of bimetallic catalytic systems, those based on substitutional solid solutions and intermetallic compounds, the segregation processes in these two types of catalytic systems, and the possibility of using these processes for fine tuning of the active site structure on the catalyst surface. The applicability of this phenomenon to control the catalytic properties in various reactions is considered separately. The Conclusion addresses the prospects for the development of this research area.

2. Adsorption-induced segregation in bimetallic systems

2.1. Different types of bimetallic systems

Since this review considers two types of bimetallic systems, substitutional solid solution and intermetallic compounds, it is necessary, first of all, to clarify what is meant by these two types of systems and what the difference between them is.[45,46] Figure 1 shows the schematic view of formation of the two types of bimetallic systems described below that conventionally consist of two different metal atoms (A and B).

A substitutional solid solution can be represented as a binary system A_xB_{1-x}, where metal A can be incorporated into the lattice of the second metal B (and occupy its sites in the crystal lattice) over a broad range of atomic ratios determined by the

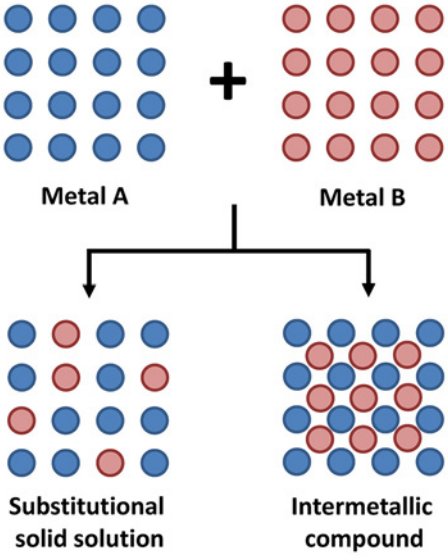

Figure 1. Schematic view of the formation of bimetallic substitutional solid solutions and intermetallic compounds at the atomic level.

solubility limit to form a mixed phase. It is important that this is not accompanied by pronounced structural transformations regarding the type of crystal lattice.[47,48] As an example, consider the PdCu alloy with 1 : 1 metal ratio and with a face-centred cubic (FCC) lattice composed of randomly alternating Pd and Cu atoms; the corresponding monometallic phases (Pd and Cu) also have the FCC structure. In this case, the single metals and the alloy have the same structure in which copper and palladium atoms occupy the same crystallographic sites in a random manner, that is, the atom alternation is stochastic. This alloy is referred to as the substitutional solid solution $Pd_{0.5}Cu_{0.5}$.[49,50]

An intermetallic compound (IMC) can be conceived as a compound of strictly stoichiometric composition A_xB_y, formed from metals A and B with a structural ordering quite different from those of the components; thus, these compounds can be referred to as atomically ordered alloys. The IMC phases have a strictly definite composition A_xB_y, where x and y are integers and the atoms alternate in a regular manner.[47,51] As an example, consider Pd and Cu, which both have FCC lattice in a pure state, but upon mixing in various proportions, they can form, under certain conditions of synthesis, Pd_1Cu_1-IMC, which has an absolutely different structure, that is primitive cubic (PC) structure corresponding to *B*2 structural type (CsCl, space group $Pm\bar{3}m$) derived from the body-centred cubic (BCC) lattice, with heteroatoms in the lattice being strictly ordered, unlike those in the substitutional solid solution $Pd_{0.5}Cu_{0.5}$ (FCC).[52,53]

The natures of the bond between two heteroatoms in these two types of bimetallic systems are also considerably different.

In substitutional solid solutions, one metal is mixed with the other one within the solubility limits to give a continuous series of compositions as a result of metal–metal bond formation between the metals.[54] The IMC formation is possible only between the elements that differ in size and considerably differ in electronegativity; otherwise, according to the Hume-Rothery rules,[55] they would form a solid solution. These rules list a set of basic conditions under which one metal can dissolve in another metal to form a substitutional solid solution:

1) the radius of the 'solute' atoms should differ from the 'solvent' atom radius by more than 15%;

2) the crystal structures of the 'solute' and the 'solvent' should be the same;

3) the highest solubility occurs when the 'solvent' and 'solute' atoms have the same valence. The greater the difference between the valences of the 'solute' and 'solvent' atoms, the lower the solubility;

4) the 'solute' and the 'solvent' should have similar electronegativities. If the electronegativity difference is too high, the metals tend to form intermetallic compounds rather than substitutional solid solutions.

Thus, according to these rules, IMC cannot be formed by two neighbouring elements in the Periodic Table.[48,56] However, it is worth noting that these rules are not laws, but they only help to predict the solubility of elements to form alloys; correspondingly, there are bimetallic systems that violate this trend. The main cause for the generation of a clearly defined periodic structure in intermetallics is the formation of an obvious covalent bond between the metal atoms that compose IMC. This nature of interaction gives rise to unique and complex crystal structures that differ from the structure of any of the initial metals, whereas in the case of substitutional solid solutions, the crystal structure of one of the initial metals (solvent) is preserved. The key features of IMCs that make them applicable for catalysis are high stability and strictly regular structure, with the electronic (ligand) and geometric (ensemble) effects, which are also considered for substitutional solid solutions, being the key factors relevant to the catalytic applications.[57,58]

Thus, it can be stated that the main differences between these two systems as regards adsorption-induced processes are their different thermodynamic stability and the absence/presence of structural ordering at the atomic level. This indicates that the systems based on substitutional solid solutions are expected to be more susceptible to the influence of the reaction medium and/or heat treatment than IMC-based systems.

2.2. Effect of CO on various types of bimetallic systems

2.2.1. Bimetallic systems based on substitutional solid solutions

As has already been noted, the surface segregation of bimetallic systems based on substitutional solid solutions by itself has been fairly long known and thoroughly studied. In this regard, palladium-based systems such as PdAg, PdAu, and PdCu are among the best known. In the literature, there are quite a few experimental and theoretical studies that discuss the surface segregation of the more reactive alloy component, palladium, in PdAu systems caused by stronger chemical bond of palladium with the adsorbate.[14,31,59–63] For example, Goodman and co-workers[14] studied the transformations that take place on the surface of a model system, the AuPd(100) single crystal, on exposure to carbon monoxide using the polarization modulation infrared reflection-absorption spectroscopy (PM-IRAS). As a result, the authors demonstrated that even at a relatively low CO partial pressure (~0.1 mbar), segregation of palladium atoms takes place to give extended sites on the surface of the bimetallic single crystal. Languille *et al.*[60] also studied the effect of submillibar (less than 1 mbar) CO pressures on the surface of a bimetallic AuPd(110) single crystal using a set of surface-sensitive techniques *in situ* such as scanning tunnelling microscopy (STM), X-ray photoelectron spectroscopy (XPS), and PM-IRAS. Analysis of the data indicated that exposure to CO is accompanied by formation of new adsorption sites, which attests to the surface segregation of palladium. Delannoy *et al.*[31] demonstrated segregation of Pd atoms for the $AuPd/TiO_2$

bimetallic catalysts in a $CO+O_2$ mixture using diffuse reflectance IR spectroscopy of adsorbed CO and transmission electron microscopy (TEM). The authors showed that the segregation of Pd atoms is accompanied by a decrease in the catalyst activity in the CO oxidation; this behaviour was attributed to the possible replacement of Au atoms in low-coordination sites by Pd atoms. Density functional theory (DFT) calculations[61] demonstrated that the relatively high CO adsorption energy on Pd is the driving force for the segregation of palladium atoms on exposure to CO. Ouyang *et al.*[63] investigated the possibility of controlling the active site structure in the $PdAu/SiO_2$ single-atom alloy (SAA) catalysts using CO-induced segregation. It was shown by the IR spectroscopy of adsorbed CO that the structure of palladium sites can be reversibly changed in the controlled manner (from isolated atoms to clusters) by varying CO treatment conditions: partial pressure and temperature. Using theoretical calculations, the same research group[64,65] predicted that the CO-induced segregation effect could be used for tuning the surfaces of other SAAs: Pd/Au(111), Pd/Ag(111), Ir/Ag(111), and Ni/Cu(111).

A series of recent publications of V.I.Bukhtiyarov's research group[29,30,66–68] is devoted to systematic study of CO-induced segregation for model bimetallic catalysts, PdAu and PdAg, in which particles of the active components are supported on the highly oriented pyrolytic graphite (HOPG) (Fig. 2). These model catalysts were investigated by *in situ* X-ray photoelectron spectroscopy (*in situ* XPS) at submillibar pressures with simultaneous control of the composition of reactants and reaction products in the gas phase (mass spectrometry).[29] This approach allowed the authors to establish the correlation between the catalytic properties and the chemical state/structure of the active component on the surface of the operating catalyst. It was demonstrated that PdAu/HOPG model bimetallic catalysts (average particle size of 5–8 nm depending on the sample; Au/Pd atomic ratio in the 0.4–0.9 range) are active in the CO oxidation at temperatures above 150°C. Under the action of the reaction mixture at temperatures below 150°C, palladium atoms segregate to the surface of bimetallic particles caused as a result of CO adsorption giving $Pd–CO_{ads}$ bonds. This assumption was confirmed by DFT calculations of the energy characteristics of reversible palladium segregation on the surface of PdAu bimetallic nanoparticles upon CO adsorption.[30] In the initial state, in the absence of carbon monoxide, the bimetallic PdAu particle in which the upper layer completely consists of gold atoms is thermodynamically more stable. The calculations of the CO adsorption energy for different sites demonstrated that palladium atoms interact with the adsorbate more strongly (1.7–2.0 eV) than gold atoms (0.1–0.2 eV). As a result, adsorption of a relatively small number of CO molecules (~10 molecules per particle composed of two hundred atoms) is

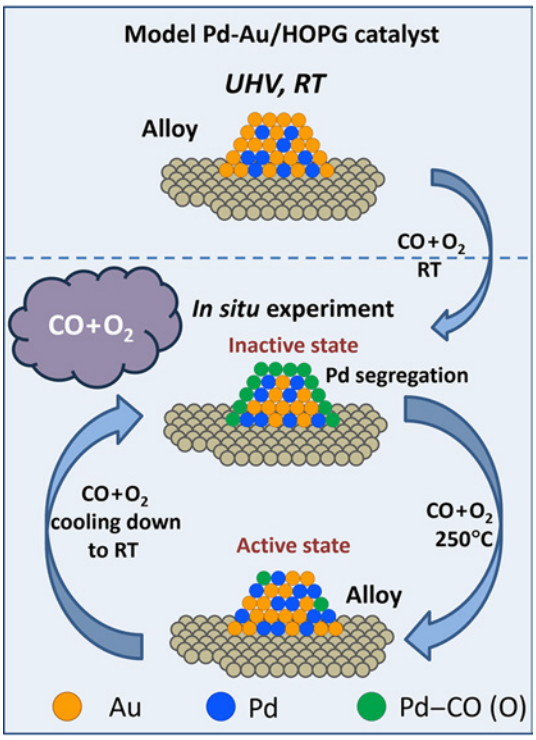

Figure 2. Schematic view of transformations of the HOPG-supported bimetallic PdAu particles taking place during CO oxidation, depending on the experimental conditions. (The Figure was created by the author using experimental data published in the Ref. 29. Copyright for the Figure belongs to the Russian Chemical Reviews). UHV is ultra-high vacuum.

sufficient to make the Pd surface segregation in HOPG-supported PdAu particles, without change in their size, energetically favourable. In the active state of the catalyst (at a temperature above 150°C), the $Pd–CO_{ads}$ bonds are cleaved upon CO desorption, resulting in the formation of PdAu alloy on the surface of bimetallic particles. It was suggested that exactly the PdAu alloy particles act as the active component in the CO oxidation. On cooling to room temperature, both a partial reversible metal redistribution along the depth of bimetallic particles and a change in their chemical state take place on the surface of the model catalyst, which attests to the reversibility of the CO-induced transformations.

A study of CO oxidation with PdAu/HOPG bimetallic catalysts with different Pd/Au ratios on the surface demonstrated that the activity depends on the initial Pd/Au atomic ratio specified at the catalyst synthesis (Fig. 3).[67] The sample with a

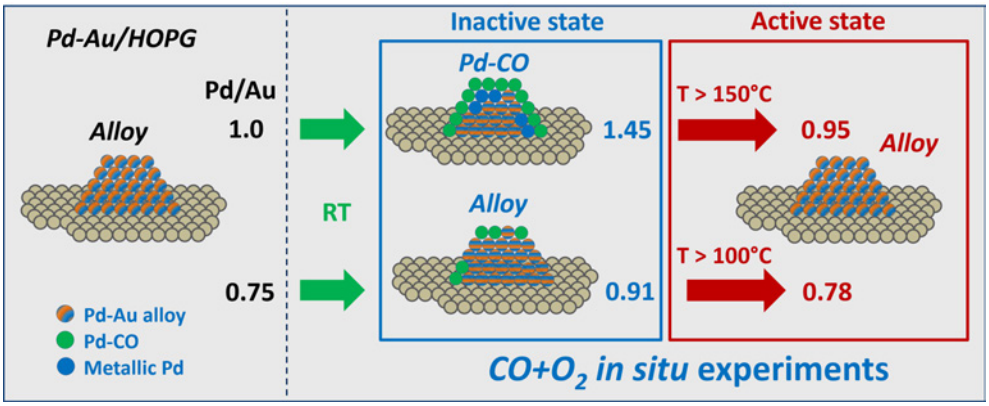

Figure 3. Schematic view of the transformations taking place on the surface of PdAu particles during CO oxidation depending on the initial metal ratio. (The Figure was created by the authors using experimental data published in the Ref. 67. The Figure Copyright belongs to the Russian Chemical Reviews.)

lower Pd/Au atomic ratio (~50.75, XPS data) on the surface showed catalytic activity even in the 100–150°C temperature range, whereas the PdAu/HOPG sample with a higher Pd/Au ratio (~1.0; XPS data) becomes active in the reaction only at a temperature of 200°C and above. The authors attributed this result to different efficiencies of the CO adsorption-induced segregation of palladium, which depends on the initial Pd/Au ratio on the catalyst surface. The lower efficiency of CO-induced segregation of Pd atoms observed for the catalyst with a lower atomic ratio may be attributed to lower CO adsorption energy on the particles formed on the catalyst surface. Indeed, recently, Sitja and Henry[69] used molecular beam method to study the adsorption of CO on bimetallic PdAu clusters containing 140±12 atoms with various metal ratios (the content of Pd atoms varied from 55 to 100%) supported on the model planar material $Al_2O_3/Ni_3Al(111)$ [alumina thin film grown on $Ni_3Al(111)$ single crystal]. The authors showed that increase in the Au surface concentration leads to a decrease in the energy of CO adsorption on bimetallic PdAu clusters. When carbon monoxide is in contact with Pd monometallic clusters, adsorption occurs on multiatomic palladium sites involving three Pd atoms. As the surface concentration of gold increases, CO starts to be adsorbed first in the bridging mode and then, as the concentration further increases, it is adsorbed linearly on the sites consisting of two and one Pd atoms, respectively. Returning to discussion of the results obtained by Bukhtiyarov *et al*.,[67] it can be stated that in the active state of the PdAu/HOPG catalyst with a higher palladium content (200°C and above), the $Pd–CO_{ads}$ bond cleavage upon CO desorption occurs simultaneously with the formation of PdAu alloy. Meanwhile, in the case of the PdAu/HOPG sample with a lower fraction of palladium, a considerable part of the PdAu alloy in the reaction mixture is located on the surface even at room temperature, probably, due to the lower energy of CO adsorption and/or insufficient quantity of accessible palladium atoms necessary to completely cover the particle surface and form $Pd–CO_{ads}$ bonds, which deactivate the catalyst.

Thus, analysis of published data provides the conclusion that the structure of the active sites of the bimetallic PdAu catalysts can be controlled by a combined use of two interrelated processes: change in the ratio between the metals at the stage of synthesis and tuning of the surface structure by using segregation effects induced by CO adsorption.

Similar studies of bimetallic PdAg/HOPG catalysts (average particle size of 6.5 nm; Pd/Ag atomic ratio of 2.5) in the oxidation of CO by a combination of *in situ* XPS and mass spectrometry techniques[68] showed that, like in the case of PdAu/HOPG samples, segregation of Pd atoms induced by CO adsorption in the reaction medium is observed even at room temperature. However, unlike the PdAu bimetallic particles, in this case, increase in the sample temperature up to 150°C enhances this effect. Considering the results, the authors assumed that the efficiency of palladium segregation induced by CO adsorption in PdAg systems is mainly determined by thermodynamic factors rather than by surface coverage with CO molecules.

Quite a few studies published in the last decades have been devoted to the transformations taking place on the surface of bimetallic PdAg catalysts during the low-temperature CO oxidation; therefore, a certain progress has been attained in the understanding of these processes.[70–76] These publications can be subdivided into two groups: those addressing real catalysts and using *ex situ* methods and those addressing bulk model systems, most often based on single crystals, and using *in situ* methods. For example, Venezia *et al*.[70] investigated CO oxidation in the presence of pumice -supported bimetallic PdAg catalysts by a combination of X-ray diffraction, *ex situ* XPS, and mass spectrometry techniques. The authors demonstrated that the catalytic activity of these systems depends on the initial Ag/Pd atomic ratio, with the catalyst activity increasing with a decrease in this ratio. In addition, the authors investigated the activity of these catalysts after oxidative (in oxygen) or reductive (in hydrogen) pretreatment. Treatment in air at high temperature resulted in the diffusion of silver atoms into the bulk of bimetallic PdAg particles and gives rise to partially oxidized palladium; simultaneously, the authors observed an increase in the catalytic activity towards CO oxidation. It was assumed that the reaction proceeds by two different mechanisms at once. According to the first mechanism, CO adsorbed on the palladium metal directly reacts with oxygen from the gas phase to form CO_2, while the second mechanism implies the reaction of CO with lattice oxygen in the oxidized PdO species due to spillover. The subsequent hydrogen reduction of the catalyst at 350°C further increases the catalytic activity; however, this is accompanied by segregation of silver atoms back to the particle surface with simultaneous formation of extended silver sites (agglomerates), which, first, do not block palladium sites and, hence, do not inhibit the reaction, and, second, can be involved in the adsorption of oxygen, and thus contribute to oxygen activation.

Strømsheim *et al*.[72] studied the variation of the surface composition of the $Pd_{75}Ag_{25}(100)$ bimetallic single crystal during the oxidation of CO. The *in situ* XPS data provide the conclusion that the effect of the reaction medium induces the surface segregation of palladium atoms. The results of quantum chemical calculations suggest that the number of palladium atoms on the surface should decrease with increasing temperature, which was confirmed by *in situ* XPS data. The fraction of Pd atoms on the surface was lower in the active state at a temperature above 270°C than in the inactive state (T < 270°C). In addition, silver existed as the PdAg alloy over the entire temperature range (only one state is manifested in the Ag3d spectrum). At room temperature, palladium atoms in the reaction medium existed in two states (according to analysis of the Pd3d photoelectron spectrum): as the alloy localized in the near-surface layers and as CO-bound palladium on the $Pd_{75}Ag_{25}(100)$ surface. As the temperature increased to ~250°C, the signal for the latter state in the Pd3d spectrum completely disappeared, which was attributed to the desorption of CO molecules.

Using *in situ* XPS and STM supplemented by DFT calculations, van Spronsen *et al*.[73] studied a model bulk bimetallic PdAg system in which Pd was deposited on the surface of the Ag(111) single crystal to form an alloy. The authors studied the transformations that took place on the surface of this system on exposure to CO and O_2. They found that the surface composition of such a bimetallic PdAg system considerably depended on the pretreatment conditions. The DFT calculations demonstrated that the Ag/PdAg/Ag(111) system in which the surface was coated with silver and near-surface layers contain PdAg alloy was most stable under ultra-high vacuum conditions (UHV). The treatment of Ag/PdAg/Ag(111) with CO (0.5 Torr) at room temperature or with O_2 (1 Torr) at 130°C induced the surface segregation of palladium. The authors suggested that the pretreatment (with CO or O_2) of the bimetallic PdAg catalysts at relatively low temperatures and pressures may activate the catalysts because of segregation of palladium atoms.

Zhao *et al*.[77] used a combination of XPS and low energy ion scattering (LEIS) spectroscopy to study the surface segregation

of the PdCu alloy in vacuum and in various gases (H_2, CO, and CO_2). It was found that, unlike the vacuum conditions in which Cu is segregated to the surface, in the presence of gases, adsorption affects the surface composition in different ways. For example, on exposure of the PdCu alloy to H_2, CO, or their mixture, the surface is depleted in copper, that is, surface segregation of palladium atom takes place, whereas treatment in CO_2 virtually does not change the alloy surface in comparison to that in vacuum. The thermodynamic model proposed by the authors explains these phenomena semi-quantitatively considering the adsorption energy as an additional driving force for palladium segregation. In a theoretical study, Padama *et al*.[78] investigated the transformation of $Cu_3Pd(111)$ on exposure to CO by the DFT method. It was found that CO adsorption causes the surface segregation of Pd atoms. The authors attributed this transformation by stronger CO–Pd interaction compared to CO–Cu, which facilitates the Pd segregation to the surface of CuPd particles. The same group of authors[79] used theoretical calculations to study the transformation of the PdCu(111) surface under the action of CO molecules and artificially modelled COH and HCO particles as adsorbates. The results provided the conclusion that the ultimate positions of palladium atoms on the surface and in near-surface layers is affected not only by the adsorbate binding energy, but also by the structure of sites preferable for the adsorption of a particular adsorbate.

It is known that from the point of view of atom ordering, in the absence of adsorbates, under UHV conditions, bimetallic systems based on substitutional solid solutions such as PdAg and PdAu are very similar, and the most thermodynamically favourable state of these systems is a nanoparticle, in which atoms of the less active metal (Au or Ag) tend to be located in the topmost layer, as demonstrated, for example, in the theoretical work by Neyman's group.[30,80] This preferential surface segregation of one metal relative to the other one in bimetallic systems is largely determined by the different surface free energies of these metals.[35,81] According to a simple empirical rule, the element with a lower surface energy segregates to the surface in vacuum. There are quite a few published studies based on both experimental data[82,83] and results of theoretical calculations[84–89] demonstrating that the surface of bimetallic PdAg systems is enriched with silver atoms under UHV. These relative arrangement of metal atoms is due to lower surface energy of silver compared to palladium.[83,84,87] The surface energy difference between Pd (~75–80 kJ mol^{-1}) and Ag (50–55 kJ mol^{-1}) is approximately 25 kJ mol^{-1},[83,90,91] which substantially exceeds the heat of mixing of the elements upon the formation of PdAg solid solution (4–5 kJ mol^{-1}).[92] As a result, the alloy surface is enriched with the element with a lower surface energy.

Eom *et al*.[93] studied the formation of core–shell structures for 45 various bimetallic combinations using molecular dynamics and Monte Carlo simulation. Finally, the authors showed that both bimetallic systems, PdAu and PdAg, tend to form core–shell structures in which the core is enriched with palladium atoms, while the shell is enriched with gold or silver atoms. Furthermore, according to the obtained results, the surface segregation effect is even more pronounced for PdAg systems than for PdAu.

According to the data reported by Mamatkulov *et al*.,[30] the adsorption of CO even up to a surface coverage of only 0.3 monolayers is sufficient for thermodynamic stabilization of the structure of bimetallic PdAu particles in which all (111) terraces are occupied by palladium atoms. Considering the fact that the energies of CO adsorption on palladium and gold/silver are ~1.5–2 eV and ~0.1–0.3 eV, respectively,[80,94] the CO-induced surface segregation of palladium atoms caused by stronger interaction of CO with palladium should also be observed in the case of PdAg-based substitutional solid solutions. Papanikolaou *et al*.[65] investigated the structural changes of highly diluted bimetallic particles based on platinum group metals using DFT. The authors found that the strong interaction between CO and one of the metals significantly affects the surface morphology of catalysts and concluded that by varying the CO pressure, it is possible to control the structure of active metal ensembles on the surface of particles such as PdAu, PdAg, and PdCu. Using the DFT method, Svenum *et al*.[95] studied the effect of the adsorption-induced segregation in the presence of various adsorbates on the surface composition of thin membranes made of PdAg alloy with silver content of ~20–25%. The authors drew the conclusion that adsorption of CO can induce segregation of palladium atoms to the surface of these systems and, hence, can change the surface composition. In this case, the adsorption-induced segregation is determined by the strong metal–adsorbate interaction; according to theoretical calculations, no changes in the valence states of atoms or in the crystal structure of the substitutional solid solution take place.

2.2.2. Bimetallic systems based on intermetallic compounds

One more type of bimetallic systems that are defined as promising catalysts are those based on intermetallic compounds. They are characterized by a high degree of atomic ordering and stability of the crystal structure and, as a consequence, high stability and reproducibility of the surface active site structure. The PdGa system, which has a high selectivity in acetylene hydrogenation, is among the best studied to date. However, the main drawback of these systems is low stability to oxidation: even on short-term storage of samples in air or on exposure to an oxidative medium, gallium and palladium oxides are formed. This is accompanied by decomposition of bimetallic particles, which, in turn, leads to degradation of catalytic properties, that is, decrease in the conversion and selectivity.[96] Regarding electronic properties (the outer electron shell), indium is similar to gallium; therefore, the use of indium instead of gallium also leads to the formation intermetallic PdIn compounds,[97] which are, however, less prone to oxidation than PdGa.

In the case of intermetallic systems such as PdGa or PdIn, exposure to CO does not induce surface changes, that is, no surface segregation of Pd or Ga takes place.[42,98] First of all, this is due to the fact that the addition of a second component, gallium or indium, sharply changes the electronic state of palladium due to formation of covalent bonds in the resulting IMC, which, in turn, affects the adsorption properties. For example, Rosenthal *et al*.[99] investigated the electronic and geometric properties of a surface model system, PdGa(111) single crystal corresponding to the B20 (FeSi) structural type, by XPS, ultraviolet photoelectron spectroscopy (UPS), STM, X-ray photoelectron diffraction, and low-energy electron diffraction (LEED). By comparing the results of UPS and temperature-programmed desorption (TPD) of chemisorbed CO for the PdGa(111) and Pd(111) single crystals, the authors were able to establish the correlation between the electronic structure and the adsorption capacity of palladium atoms. It was shown that CO desorption from Pd(111) takes place at a temperature of approximately 240°C, while in the case of PdGa(111), CO is completely desorbed even at –10°C. The authors attributed this

pronounced difference in the desorption temperature (250°C) to a sharp change in the electronic structure of palladium atoms. Thus, the presence of covalent bonds and the formation of a different crystal structure in IMC increases the density of states (DOS) in the outer levels (that is, leads to a higher degree of filling of d states), which gives rise to a partial negative charge on palladium atoms and, hence, changes the adsorption capacity. In other words, the energy of CO adsorption on palladium atoms in PdGa-IMC is significantly lower than that for monometallic palladium. Similar results were obtained in other studies,[51,100] in which the authors found a shift in the density of states upon the formation of PdGa intermetallic, which resulted in a change in the adsorption properties. For example, according to Kauppinen and Grönbeck,[100] CO adsorption on PdGa gets weaker (–1.07 eV) compared with the palladium metal, for which this value is –1.5 to –1.6 eV. This may account for the stability of this system to CO-induced segregation of palladium atoms. The PdIn intermetallic is a close analogue of PdGa.[43] It is also known that the electronic state of palladium in these systems changes in a similar way upon the addition of In or Ga compared to that of monometallic palladium.[101] In our studies of model systems in which PdIn nanoparticles were supported on HOPG, carried out by XPS and STM,[42,102] we found that a thin intermetallic layer is already formed on the surface of bimetallic particles in the stage of thermal vacuum deposition of the second metal (indium) on the monometallic Pd/HOPG. The binding energy of the principal $Pd3d_{5/2}$ line in the XPS spectra shifts to higher values by 0.9 eV and amounts to 336.5 eV, which attests to the generation of a local charge on the palladium atoms caused by the formation of a clear-cut covalent bond in the intermetallic compound. Like in the case of PdGa, the electronic properties of palladium markedly change. Thus, the PdIn stability to CO adsorption demonstrated by Fedorov *et al*.[42] in relation to PdIn/HOPG may be attributable not only to the higher stability of the PdIn intermetallic structure, but also to decreasing energy of carbon monoxide adsorption or, in other words, to weakening of the interaction between CO and palladium compared to that observed in monometallic palladium or PdAu or PdAg type substitutional solid solutions.

It is noteworthy that no such drastic changes in the electronic properties of palladium are observed upon the addition of silver atoms.[103] In a recent paper,[104] the local structure of single Pd_1 sites on the surface of α-Al_2O_3-supported Pd_1In_1 intermetallic nanoparticles was studied by a combination of IR spectroscopy of adsorbed CO and DFT. The CO adsorption energies for various Pd and PdIn-IMC surface sites found by DFT calculations are summarized in Table 1.[104] According to calculations, CO is not adsorbed on indium atoms; adsorption occurs only on Pd sites. It can be seen from these data that the energy of CO adsorption on the PdIn-IMC surface is much lower than that on the monometallic palladium surface. The energy of CO bridge adsorption on the (110) face is low (–0.09 eV). This accounts for the fact that this absorption band was not observed in experimental diffuse reflectance IR spectra of CO. This low adsorption energy as compared with the CO bridge adsorption on monometallic palladium (–1.51 to –1.71 eV, see Table 1) is attributable to different geometries of Pd_2 sites in PdIn(110) and Pd metal. In the case of Pd metal, the distance between the neighbouring Pd atoms is 2.8 Å, whereas for PdIn(110), this distance is 3.35 Å.

Meanwhile, the lower tendency for CO-induced Pd segregation observed in the case of PdIn-IMC can be attributed to higher strength of the Pd–In bond compared to Pd–Au bond (as an analogue of Pd–Ag). Indeed, analysis of the reported bond energies that were calculated for stoichiometric PdIn-IMC[105] and PdAu solid solutions of various compositions[106] provides the conclusion that the Pd–In bond energy (–0.44 eV or –42.5 kJ mol^{-1}) is much greater than the Pd–Au bond energy (from –0.25 eV/–24.1 kJ mol^{-1} to –0.31 eV/–29.9 kJ mol^{-1}, depending on the ratio of the metals).

Table 1. Energy of CO adsorption and positions of IR absorption bands for various surface sites of Pd and PdIn-IMC according to DFT calculation results and experiments.[104]

Surface	Type of adsorption (site)	E_{ads}, eV	ν(CO), cm^{-1}	
			DFT calculations	experiment
Pd(111)	Linear	–1.17	2092	2086
Pd(111)	Bridge	–1.51	1925	1942
Pd(111)	Threefold coordination	–1.62	1848	1896
Pd(100)	Linear	–1.33	2122	not detected
Pd(100)	Bridge	–1.71	1949	1977
Pd(100)	Threefold coordination	–1.58	1756	not detected
PdIn (110)	Linear	–0.39	2058	2055
PdIn (110)	Bridge	–0.09	–	not detected
PdIn(111)	Threefold coordination	–0.77	2065	2064

One should also bear in mind the 'kinetic' stability of intermetallic structures to segregation processes, which is usually determined by diffusion barriers.[35] The bond between the Pd and In atoms in IMC is predominantly covalent, as was shown previously for various Pd-containing intermetallics by calculating the electron localization function (ELF).[43,51,107] From this, it follows that for the diffusion to the surface, Pd atoms must overcome a relatively high activation barrier caused by the requirement of cleavage of the Pd–In bonds, which are essentially covalent in this case. If the path of Pd atoms towards the surface of PdIn IMC is represented as a series of jumps over vacancies, then each jump is the displacement of a Pd atom either to an indium vacancy or to a palladium vacancy. However, in the case of IMC, indium vacancies are specific to indium atoms and, therefore, they are poorly accessible for Pd atoms for energy reasons, while palladium vacancies are rather remote from Pd atoms, which are mainly surrounded by indium, since the structure of intermetallic is ordered;[65] hence, the diffusion of Pd is hindered in this case. In Pd-based substitutional solid solutions with random distribution of Pd atoms, the migration of Pd atoms *via* Pd vacancies is facilitated because there are more neighbouring sites that are expected to be occupied by atoms of the same type; therefore, the surface segregation of Pd atoms occurs much more easily.

2.2.3. Effect of CO (generalization)

The above analysis of the available literature provides the conclusion that CO is, beyond doubt, promising to be used as a tool for fine tuning of the surface in bimetallic catalysts based on substitutional solid solutions such as PdAu, PdCu, and PdAg. For this purpose, it is necessary to take into account the initial ratio of the metals (specified at the stage of synthesis) in the bimetallic system and to vary the conditions of CO treatment (partial pressure, temperature). Catalysts based on intermetallic compounds are stable on exposure to CO.

2.3. Effect of O_2 on various types of bimetallic systems

2.3.1. Bimetallic systems based on substitutional solid solutions

It is known that oxygen treatment of bimetallic systems based on substitutional solid solutions such as PdAg or PdAu can also induce the surface segregation of Pd;[71,108–111] However, in this case, segregation is accompanied by the formation of surface palladium oxide. For example, Guesmi *et al.*[108] used DFT calculations to investigate the segregation energies of isolated palladium atoms in the PdAu(111) alloy depending on the surface coverage with oxygen. It was found that 0.3 oxygen monolayers are sufficient to induce palladium segregation to the surface; analysis of the density of d-states showed that this is due to the high oxygen affinity of palladium, *i.e.*, the segregation is accompanied by the formation of a strong Pd–O bond. Theoretical calculations for the oxygen-induced segregation of palladium on the $Ag_3Pd(111)$ and $Au_3Pd(111)$ surface[109,110] demonstrated that the manifestation of these effects directly depends on the composition of the reaction medium. When the oxygen content is low (nearly UHV conditions), the Pd segregation is hindered, since at higher pressure, the segregation should give a stable oxidized palladium species. Golio and Gellman[111] studied the oxygen activation of Ag_xPd_{1-x} bimetallic films with different compositions towards ethylene hydrogenation. The authors also demonstrated the surface segregation of palladium *via* the formation of the oxidized palladium phase on the surface. For example, for PdAg, these changes in the surface structure caused by the treatment with oxygen are consistent with thermodynamic data. Indeed, the Gibbs energy of formation of the oxide $\Delta G_f(PdO)$ is –115.6 kJ mol^{-1},[112] while for silver oxide, $\Delta G_f(Ag_2O)$ = –31.0 kJ mol^{-1}. This provides the conclusion that in substitutional solid solutions such as PdAg, first of all, palladium oxidation takes place and only after that, silver oxide is formed. Therefore, treatment with oxygen can hardly be applicable for fine tuning of the surface active sites in the systems based on substitutional solid solutions. In the reactions that involve oxygen, the surface is spontaneously adjusted to the reaction conditions (oxygen deficiency/excess, temperature), and in the case of hydrogenation, for example, selective hydrogenation of the C≡C bond, palladium must be first reduced, which is likely to yield extended palladium ensembles on the surface and, hence, would lead to the loss of the advantages of bimetallic systems. Thus, it can be stated that the surface of bimetallic catalysts based on substitutional solid solutions cannot be controlled by treatment with oxygen. Therefore, this issue is not discussed below.

2.3.2. Bimetallic systems based on intermetallic compounds

The selective catalytic hydrogenation is the most efficient way to remove acetylene and its homologues from olefin feedstock in order to achieve polymerization purity (~1 ppm). In industry, this is done using Pd-containing catalysts; however, despite the high activity, these catalysts lose their selectivity at high conversions of acetylene, that is, complete hydrogenation to ethane takes place. This is attributed to the presence of extended Pd sites (Pd_n where $n > 2$) on the surface of monometallic palladium catalyst. The IMC-based systems are promising catalysts for selective hydrogenation of C≡C bond to C=C bond, as they are distinguished by a high degree of ordering and crystal structure stability and, hence, by high stability and reproducibility of the active site structure on the sample surface.[45,113] Among these catalysts demonstrating exceptionally high selectivity in the acetylene hydrogenation, PdGa has been most studied.[114–116] However, this catalyst has a low oxidation stability, and even a short-term storage of the catalyst in air leads to formation of an oxide of more active metal (gallium); this is accompanied by degradation of bimetallic particles, which decreases their activity and selectivity.[117] Since indium resembles gallium in the electronic structure, and, in addition, PdIn-based catalysts are more stable to oxidation,[97,113] these systems also have a great potential as catalysts in the selective hydrogenation of unsaturated hydrocarbons.[118,119] Catalysts based on PdIn demonstrate high efficiency in a number of other important reactions such as reduction of nitrates,[120] steam reforming,[121] hydrogenation of CO_2 to methanol,[122,123] *etc*. Most researchers agree that the catalytic properties of these systems are determined by both the geometric arrangement of metal atoms and the electronic properties of intermetallic particles. For example, the catalytic activity and selectivity to CO_2 in the steam reforming of methanol markedly depend on both the Pd : In ratio and the total amount of the metals.[121] The high selectivity of $PdIn/Al_2O_3$ catalysts to CO_2 is caused by the formation of the PdIn alloy, while palladium metal, which does not form bonds with indium, is in charge of the selectivity to CO. García-Trenco *et al.*[122] showed that the rate of methanol formation in the hydrogenation of CO also depends on the Pd : In atomic ratio. For example, excess palladium in the catalyst (Pd : In ratio > 1 : 1) leads to a decrease in both methanol selectivity (50%) and catalyst activity. The catalyst with PdIn intermetallic particles (Pd : In = 1 : 1) deposited on the surface is most active in this reaction. It is obvious from the above that the activity of these IMC-based systems directly depends on the surface structure and the electronic state of metals present on the surface.

As has already been noted, treatment of PdIn or PdGa-IMC systems with oxygen at elevated temperature results in the predominant oxidation of the component that has a higher oxygen affinity, that is, indium (or gallium); this makes it possible to form surface structures with adjacent metal (Pd) and metal oxide domains and $Pd@M_2O_3$ core–shell systems (where M = In or Ga). Although this process is often called adsorption-induced segregation, like that observed on contact of CO with substitutional solid solutions, the nature of this process is fairly different. The IMC structure is destroyed as a result of selective oxidation of the oxophilic In(Ga) component (corrosive chemisorption), which leads to its migration to the nanoparticle surface to give the surface oxide. The structural changes of IMC affect both the particle surface and bulk *via* removal of the oxophilic component from IMC. Thus, the oxidative surface treatment of these systems can be used as a tool for fine tuning of the active site structure. Nevertheless, only a few publications are devoted to the possibility of deliberate control of the surface structure of PdIn-IMC-based catalysts by redox treatment.[102,124,125] Bukhtiyarov *et al.*[102] studied the effect of oxygen on the model PdIn/HOPG catalysts (the average particle size depending on the sample was 4.1–4.2 nm; the In/Pd atomic ratio was in the 0.35–1.0 range) by *ex situ* XPS. The experiments were carried out in a high-pressure cell; this made it possible to pretreat the samples with various gases at pressures of up to 1 bar and at temperatures ranging from room temperature to 500°C and then to measure the XPS spectra without intermediate contact of the samples with air. The oxidative treatment was carried out at 200 mbar O_2 pressure at two temperatures: room temperature and 100°C. It was shown that this mild oxidative

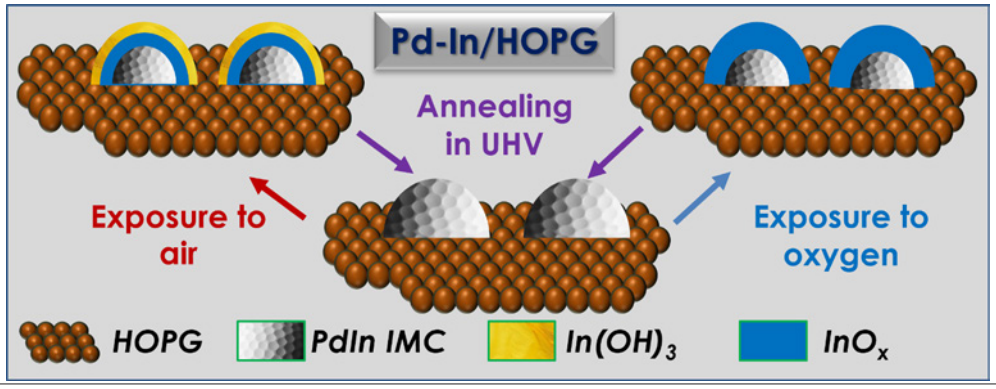

Figure 4. Schematic view of the evolution of PdIn intermetallic particles on the HOPG surface depending on the type of treatment. (The Figure was created by the authors using experimental data Published in the Ref. 124. The Figure Copyright belongs to the Russian Chemical Reviews.)

treatment of PdIn/HOPG led to partial oxidation of In, thus causing its segregation to the surface of PdIn nanoparticles. This was also accompanied by changes in the $Pd3d_{5/2}$ spectrum: an additional state with binding energy of 335.7 eV, which is characteristic of Pd metal, appeared even at room temperature. Therefore, the authors concluded that PdIn-IMC partially decomposed. The observed changes in the PdIn surface structure caused by indium oxidation/segregation are consistent with thermodynamic data: $\Delta_f G\,(In_2O_3) = -926.4$ kJ mol^{-1} and $\Delta_f G\,(PdO) = -115.6$ kJ mol^{-1}.[112] The subsequent heating of the sample in vacuum at 500°C led to the back redistribution of metals on the surface (the In/Pd atomic ratio on the surface decreased to the initial value) and to complete restoration of the $PdIn_{IMC}$ structure.

Panafidin *et al.*[124] also studied the model PdIn/HOPG bimetallic catalysts by a combination of scanning tunnelling microscopy and synchrotron radiation X-ray photoelectron spectroscopy (SR XPS), in particular in the *in situ* mode. The main goal was to elucidate the particle structure and the composition and chemical state of the particle surface after long-term storage in air and to study the nanoparticle evolution during treatment in O_2 in the submillibar pressure range at elevated temperature. According to SR XPS data, long-term storage of PdIn/HOPG catalysts in air leads to almost complete decomposition of IMC, with the sample surface being strongly enriched with indium, which segregates to the surface upon oxidation to give surface indium hydroxide and subsurface indium oxide uniformly distributed over the depth of Pd^0. The successive heating of the samples under ultra-high vacuum is accompanied by a gradual decrease in the In/Pd ratio for all samples, and after sample heating at 500°C, the In/Pd ratio virtually coincides with that for freshly prepared samples, which attests to the back metal redistribution in the particle; as a result, metal distribution over the depth becomes more uniform; Pd and In are completely incorporated into IMC, which attests to complete restoration of IMC structure under these conditions. According to the results of *in situ* XPS, mild oxidative treatment with O_2 (0.25 mbar) at 150°C results in indium segregation (the In/Pd atomic ratio increases), and the resulting oxide InO_x is uniformly distributed over the PdIn particle depth. Meanwhile, treatment with oxygen at 200°C leads to enrichment of the particle surface with this oxide. Treatment of PdIn samples under more drastic oxidative conditions (long-term storage in air or O_2 treatment at higher temperatures or pressures) gives rise to the surface indium oxide and/or hydroxide, which presumably fully blocks the active surface of bimetallic particles (Fig. 4).

In relation to the PdIn/HOPG model catalysts, it was demonstrated[102,124] that the adsorption-induced segregation caused by the treatment of these systems with oxygen can be used to change the surface composition by varying both the oxygen pressure and the treatment temperature. Thus, this approach can serve for targeted tuning of the surface structure of PdIn catalysts (by O_2 pretreatment) in order to attain the best catalytic performance (catalytic activity/selectivity relationship) in a particular reaction.

Smirnova *et al.*[125] studied the transformations occurring in the bulk and on the surface of Al_2O_3-supported PdIn intermetallic particles during reductive and oxidative treatment. According to the results of IR spectroscopy of adsorbed CO and extended X-ray absorption edge fine structure (EXAFS) and X-ray absorption near-edge structure (XANES) techniques, the reduction of the initial sample (after contact with air) with H_2 at 500°C gives rise to intermetallic PdIn nanoparticles with a uniform Pd and In distribution. IR spectroscopy of adsorbed CO showed that oxygen treatment at 25°C for 30 min leads to partial decomposition of PdIn-IMC to give Pd^0 on the surface (~29%). As the temperature of oxidative treatment was raised to 250°C, the fraction of Pd^0 increased (~62%), and the spectrum did not exhibit absorption bands typical of PdO. Considering the EXAFS and XANES data, the authors concluded that the reductive and oxidative treatments give neither In^0 nor PdO. Also, according to EXAFS and XANES data, in the initial sample, ~65% of indium occurs as In_2O_3 and ~52% of palladium occurs as Pd^0, and after reduction with hydrogen, they are completely incorporated in PdIn-IMC. The oxidative treatment at room temperature and at 250°C induces partial decomposition of PdIn-IMC to give palladium metal and indium oxide, the fractions of which amount to ~21 and ~40% (at 25°C) and ~45 and ~66% (at 250°C), respectively. On the basis of the results, the authors concluded that the oxidative treatment gives rise to core–shell particles, with the core being composed of In-depleted PdIn-IMC, apparently with a Pd^0 inner core, and the shell being a mixture of Pd^0, In_2O_3, and a small amount of PdIn-IMC (Fig. 5).

2.3.3. Effect of O_2 (generalization)

The above analysis of the available literature considering PdIn catalysts provides the conclusion that the adsorption-induced segregation phenomenon caused by the oxygen treatment of IMC-based bimetallic systems can be used to change the surface composition by varying both the oxygen pressure and the treatment temperature.

3. Adsorption-induced segregation as a way to control the composition of the catalyst surface

Despite the fact that numerous publications are devoted to the segregation phenomenon, the deliberate use of this phenomenon

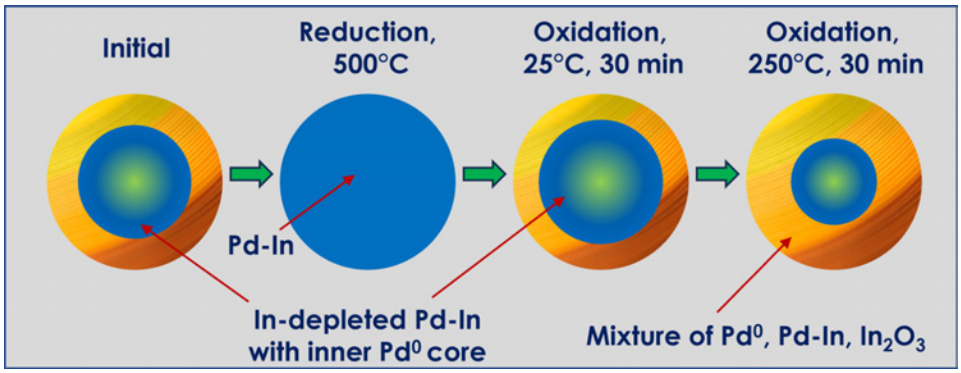

Figure 5. Preliminary models of supported PdIn nanoparticles after the reductive and oxidative treatments of the $PdIn/Al_2O_3$ catalysts.[125]

for fine tuning of the surface composition and morphology and, hence, for the formation of various types of active sites in bimetallic catalysts receives virtually no attention. Nevertheless, this approach has a great potential for practical application, as evidenced by the increasing number of studies addressing the use of adsorption-induced segregation in the post-synthetic modification of active site structure of bimetallic catalysts to achieve the optimal catalytic performance (activity and selectivity).

The applicability of this approach was demonstrated by Anderson and co-workers.[37,38] In particular, the authors ascertained that the CO-induced segregation can be used to enhance the performance of the $PdCu/Al_2O_3$ catalysts in the selective hydrogenation of the C≡C bond. The conditions required for the surface segregation of palladium atoms were determined by diffuse reflectance IR spectroscopy of adsorbed CO. In the case of the $PdCu_{10}/Al_2O_3$ sample, the fraction of the single-atom Pd surface sites increased from 4% to 5.3%, and also dimeric Pd–Pd sites (5.7%) appeared. As a result, the catalyst activity in the selective acetylene hydrogenation to ethylene increased (acetylene conversion measured at 50°C increased from 96 to 100%). In the case of the $PdCu_{25}/Al_2O_3$ sample, the fraction of single-atom Pd sites increased from 2% to 5.6%, but dimeric sites on the surface were virtually absent (<0.2%), and the catalyst activity also increased (acetylene conversion measured at 50°C increased from 29 to 70%). The achieved beneficial effects were retained throughout the whole catalytic process, indicating that the active sites formed on the surface upon CO adsorption are rather stable under reaction conditions.

Ouyang *et al.*[63] demonstrated the possibility of controlling the active site structure in the $PdAu/SiO_2$ SAA catalysts (ranging from single atoms to clusters) by using CO-induced segregation. These sites were found to have different selectivity in ethanol dehydrogenation. When SAA structures (single-atom sites) predominated on the surface, high selectivity to acetaldehyde (100%) was observed. In the case of clusters, CO treatment of the sample induced an increase in the activity (the conversion measured at 300°C increased from 20 to 90%), but the selectivity to acetaldehyde decreased down to ~60%. Thus, the authors demonstrated that CO treatment of the sample can provide control over the reaction pathway by tuning the active site structure.

The influence of pretreatment of $PdAg/Al_2O_3$ catalysts with H_2 or CO on their behaviour in the formaldehyde and CO oxidation was studied by Meng *et al.*[126] The main investigation methods included specific surface area determination by the Brunauer–Emmett–Teller (BET) method, X-ray diffraction, XPS, and O_2-TPD. It was found that the pretreatment leads to surface reconstruction, resulting in increasing amount of active oxygen and, as a consequence, higher activity of the catalysts in both mentioned reactions: in the formaldehyde oxidation, the conversion at 40°C increased from 30 to 80%, while in the CO oxidation, the conversion at 80°C increased from 20 to 90%. Thus, treatment with CO was more efficient than the treatment with hydrogen.

Shetty *et al.*[127] showed that the performance of PdAu nanowires in the electrocatalytic oxidation of methanol can be improved *via* CO-induced segregation of palladium atoms. In the case of bimetallic nanowires pretreated by heating in CO, the reaction potential decreased, which is due to higher Pd content on the surface; meanwhile, the specific activity of the catalyst did not change. The authors also performed DFT calculations, which were in good agreement with the experimental data. Thus, it was shown that it is possible to develop a strategy for independent control of the reaction potential and nanocatalyst activity *via* the use of adsorption-induced segregation.

The applicability of the adsorption-induced segregation effect based on CO treatment for enhancing the performance of $PdAg/Al_2O_3$ catalysts in the selective hydrogenation of acetylene to ethylene was demonstrated by Stakheev and co-workers.[128,129] The relationship between the spectroscopic data on the surface structure and the performance of the $PdAg_3/Al_2O$ and $PdAg_2/Al_2O_3$ catalysts was established by IR spectroscopy of adsorbed CO and XPS, in particular in the *in situ* mode. As a result, it was shown that sample pretreatment with CO markedly increases the catalytic activity. Complete conversion of acetylene over freshly reduced catalyst was achieved at ~150°C, while in the case of the CO-pretreated sample, this already occurred at 125°C, with the selectivity to ethylene remaining the same. The results of IR spectroscopy of adsorbed CO and XPS indicated that the observed increase in the catalytic activity is attributable to surface enrichment of bimetallic PdAg particles with palladium atoms and to partial transformation of Pd_1 isolated sites into Pd–Pd dimers as a result of CO-induced segregation. It is noteworthy that CO-induced segregation leads to the formation of only Pd_2 active sites, but there is no formation of larger ensembles of three or more neighbouring Pd atoms, which are expected to markedly decrease the catalyst selectivity to ethylene. An *in situ* XPS study of the $PdAg_2/Al_2O_3$ catalyst[129] showed that treatment with CO results in a considerable segregation of Pd atoms to the surface of bimetallic particles. This specific configuration of particles in which the surface is enriched with palladium atoms is also quite stable without CO. The reduction with hydrogen at 450°C restores the initial structure of the nanoparticle surface. It is important that the modified surface remains stable throughout the reaction. Note that acetylene hydrogenation in *in situ* experiment proceeded only by the selective hydrogenation pathway, *i.e.*, the selectivity to ethylene was 100%, which is not surprising considering the

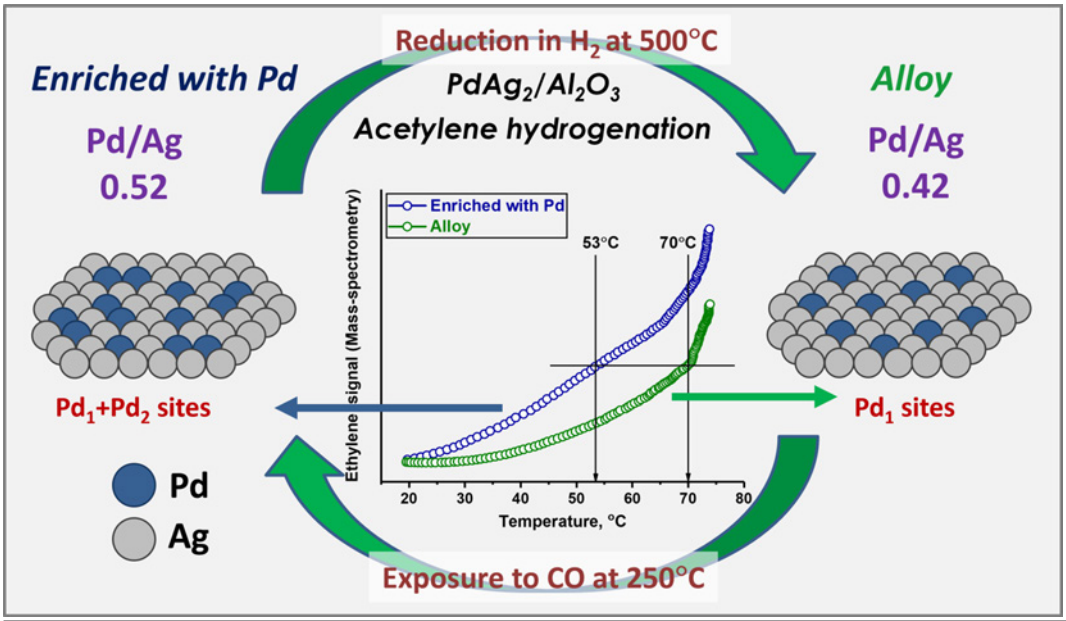

Figure 6. Schematic view of the relationship between the catalytic properties and changes in the PdAg catalyst surface that take place upon CO-induced segregation. (The Figure was created by the authors using experimental data published in the Ref. 129. The Figure Copyright belongs to the Russian Chemical Reviews.)

low acetylene conversion (~20%). The relationship between the catalytic properties and changes in the PdAg catalyst surface that take place as a result of CO-induced segregation are schematically depicted in Fig. 6. It can be seen that the pretreatment of the $PdAg_2/Al_2O_3$ catalyst with CO results in increasing catalytic activity. Equal partial pressures of C_2H_4 were observed at ~70°C and 53°C for the freshly reduced and CO-treated catalyst, respectively, which means that the catalytic activity is much higher in the latter case. These results clearly demonstrate that the adsorption-induced segregation can actually be used as a tool for fine tuning of the surface of PdAg bimetallic catalysts and, hence, for controlling the catalytic performance *via* targeted formation of certain types of palladium active sites. The optimal conditions of CO treatment to attain the most pronounced enhancement of the performance of these bimetallic catalysts include a temperature in the 200–250°C range and a broad pressure range from a few to a few hundred mbar.

The same research group[130,131] reported data on the applicability of segregation induced by adsorption of O_2 for fine tuning of the surface of bimetallic PdIn nanoparticles supported on alumina to improve the catalytic performance (activity, selectivity) in the selective hydrogenation of diphenylacetylene (DPA). Diffuse reflectance IR spectroscopy of adsorbed CO and XPS, including *in situ* mode, were also used to correlate the spectroscopic data on the surface structure and the catalytic performance of $PdIn/Al_2O_3$ (2.5% Pd–2.7% In). The redox treatments were carried out over a wide range of temperatures (from room temperature to 500°C) and oxygen pressures (from a few to a few hundred mbar). According to the results of catalytic experiments, the O_2-induced segregation can be used for the targeted controlled and reversible tuning of the catalytic performance (activity/selectivity) of the $PdIn/Al_2O_3$ intermetallic catalyst in the selective hydrogenation of DPA. After the reduction with hydrogen at 500°C, the $PdIn/Al_2O_3$ catalyst had an exceptionally high selectivity to stilbene (~98%), but a relatively low activity in this reaction. A mild oxidative treatment with oxygen in the temperature range of 25–150°C increased the activity several-fold, but the selectivity somewhat decreased. The oxidative treatment under more drastic conditions (250°C) led to a sharp increase in the hydrogenation rate by more than an order of magnitude. However, the increase in the activity was accompanied by a significant loss of the selectivity to stilbene from ~97 to ~82%. The observed changes in the catalytic performance were shown to be fully reversible in the repeated oxidation and reduction cycles; hence, the O_2-induced segregation can be used to tune the properties of the catalyst to achieve an optimal activity/selectivity balance. Detailed analysis of the data obtained by studying the $PdIn/Al_2O_3$ catalyst using a combination of *in situ* XPS and IR spectroscopy of adsorbed CO allowed the authors to distinguish several clear-cut stages of transformation of PdIn nanoparticles during the reductive or oxidative treatment depending on temperature and, hence, to propose interpretation for the reversible changes in the catalytic performance caused by these types of treatment.[131] The schematic view of the evolution of palladium sites on the surface of Al_2O_3-supported PdIn particles depending on the treatment conditions is shown in Fig. 7. The hydrogenation of DPA over the pristine $PdIn/Al_2O_3$ catalyst (after long-term storage in air) apparently occurs on the Pd^0 and Pd-IMC active sites; in this case, monometallic Pd^0 predominates on the surface. The observed decrease in the catalytic activity after the reduction with hydrogen at 500°C is caused by the transformation of a mixture of different Pd sites (Pd^0, Pd-IMC) into Pd_1In_1 intermetallic nanoparticles, in which palladium mainly exists as isolated sites. The authors attributed the decrease in the catalytic activity to electronic and geometric effects. The increase in the activity after mild oxidative treatment (at 25 and 100°C) is presumably caused by two factors: (1) transformation of a part of the isolated monoatomic Pd_1 sites into multiatomic Pd_n sites and (2) change in the electronic state of Pd atoms due to decrease in the number of neighbouring indium atoms as a result of their 'oxidative leaching' and replacement of In atoms by Pd atoms. The oxidative treatment of the $PdIn/Al_2O_3$ catalyst at 150–250°C induces more pronounced changes in the structure of metal particles, particularly, almost complete degradation of intermetallic PdIn particles. Therefore, DPA hydrogenation mainly occurs on multiatomic Pd^0 sites, which provide a higher activity, but a lower selectivity to the olefin, as in the case of monometallic Pd catalyst. The catalytic properties of the $PdIn/Al_2O_3$ catalyst reduced once again are identical to those observed for the catalyst after the first reduction, indicating the reversibility of all changes that occur during redox treatments.

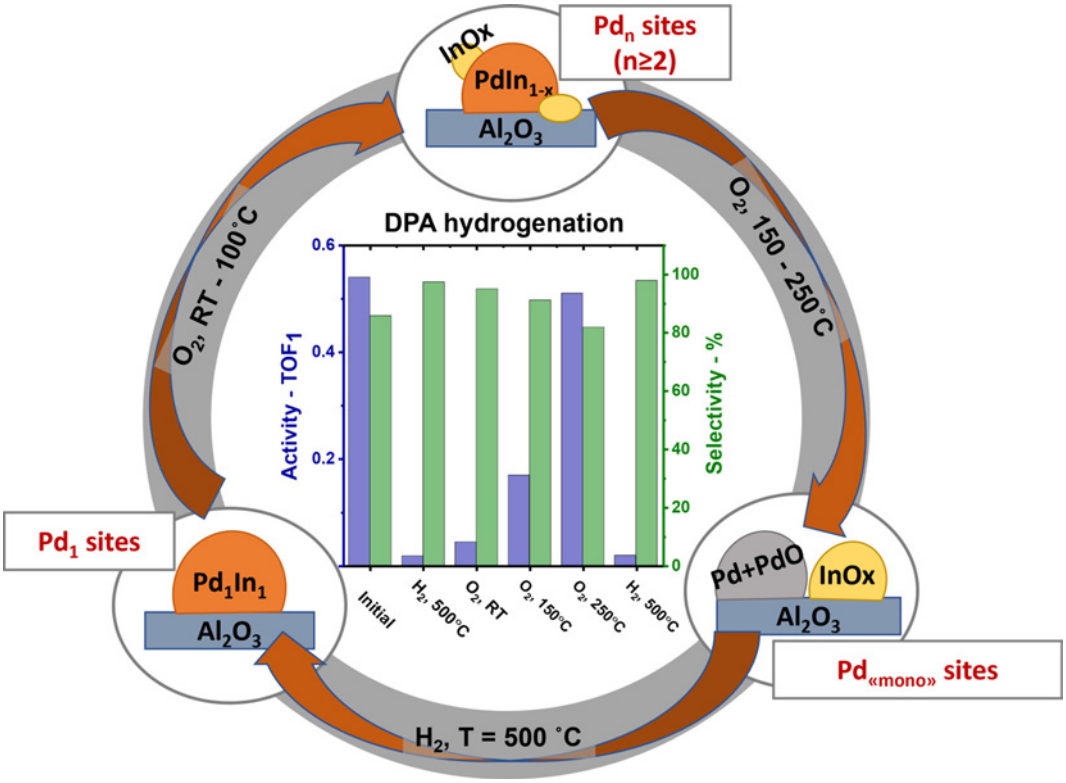

Figure 7. Schematic view of the evolution of palladium sites on the surface of Al_2O_3-supported PdIn particles depending on the treatment conditions. (The Figure was created by the authors using experimental data published in the Ref. 131. The Figure Copyright belongs to the Russian Chemical Reviews.)

Thus, the above material indicates that the rational use of the adsorption-induced segregation as a tool for fine tuning of the surface structure and optimization of the catalytic properties of various bimetallic systems deserves very close attention.

4. Conclusion. Prospects for development

The published data surveyed in this review suggest the following ways to control the active site structure in bimetallic systems: (1) variation of the ratio of metals at the stage of catalyst synthesis; (2) variation of the temperature of post-synthetic annealing of the catalyst; (3) use of adsorption-induced segregation. It can be stated that the adsorption-induced segregation can be successfully used to generate sites with a definite structure in palladium-based bimetallic catalysts such as PdAg, PdAu, PdCu, and PdIn. This, in turn, makes it possible to optimize the catalytic performance of these systems in various reactions such as selective hydrogenation of triple C≡C bond. The studies of these effects for bimetallic catalytic systems are focused on the use of surface-sensitive methods *in situ*, for example, XPS and diffuse reflectance IR spectroscopy. It should be noted that these methods are mutually complementary: XPS provides detailed information on the chemical composition and structure of the surface during the reaction or catalyst treatment in the gas phase, while diffuse reflectance IR spectroscopy provides data on the structure of active sites on the surface of bimetallic particles. Using this approach, it is possible to obtain detailed information on the evolution of the active component in these catalysts depending on the treatment conditions, which, in turn, gives information on the structure of the most effective sites involved in the reaction. As a result, it is possible to develop a strategy for selecting the pretreatment conditions for these systems in order to attain the optimal catalytic properties in a particular reaction.

A reasonable further development of research in this area may be the multi-parameter optimization of the catalysts by varying the metal ratios together with using the adsorption-induced segregation effect.

In the case of catalytic systems based on substitutional solid solutions, so-called highly dilute alloys have been gaining popularity among researchers.[41,132–136] These systems are bimetallic alloys consisting of an inert metal (for example, Cu, Au, or Ag) and a minor amount of an active platinum group metal. Catalysts based on dilute alloys are very important for industry, as they exhibit high activity and selectivity in a wide range of reactions, with the content of the expensive component being minimized. The above examples suggest that for further optimization of catalysts, it is necessary to move towards decreasing palladium content with simultaneous selection of conditions for implementation of the most significant beneficial effects of the CO-induced segregation of palladium on the catalytic performance in various reactions. For example, Markov *et al.*[137] recently demonstrated the efficiency of using the CO-induced segregation to enhance catalytic performance of the Pd_1Ag_{10}/Al_2O_3 SAA catalyst in the selective hydrogenation of acetylene to ethylene.

In the case of intermetallic PdIn systems, an interesting line of research that receives considerable attention in the literature is investigation of catalysts with a stoichiometry other than 1 : 1 and the effect of pretreatment with oxygen under various conditions on the catalytic activity. In addition, in a recent publication,[138] another approach was proposed to control the active site structure on the surface of $PdIn/Al_2O_3$ intermetallic catalysts. In order to change the structure of Pd active sites, the authors proposed to carry out reduction of the pre-oxidized catalyst surface (*e.g.*, after long-term storage in air), instead of using oxidation of the catalyst surface with oxygen. As a result, it was shown that variation of the reduction conditions may give any intermediate active site structure/combination ranging from completely oxidized Pd and In and up to PdIn-IMC with isolated Pd sites on the surface. This alternative method of surface modification may help to produce an optimal catalyst for

selective hydrogenation. Furthermore, this way of controlling the surface composition can be transferred to other similar systems such as PdGa.

Systematic research of this type should end in the elaboration of an integrated strategy for the generation of an active site structure on the surface of Pd-containing bimetallic catalysts based on the combined use of the adsorption-induced surface segregation of the active component and optimization of the composition of bimetallic nanoparticle. This method for the control of catalytic performance is completely zero-waste and, if implemented in industry, this will allow targeted modification of the properties for a catalyst that has already been loaded into the catalytic reactor; this may markedly increase the efficiency of some industrial processes. In addition, the adsorption-induced segregation and the understanding of the involved processes can be used not only for tuning of the catalyst active surface, but also for catalyst regeneration, thus increasing the service life of expensive catalysts.

This work was supported by the Ministry of Science and Higher Education of the Russian Federation (Agreement No. 075-15-2022-263). The investigations were performed using large-scale research facilities 'EXAFS spectroscopy beamline' at the Siberian synchrotron and terahertz radiation center.

5. List of abbreviations

BCC — body-centred cubic lattice;
BET — Brunauer–Emmett–Teller determination of the specific surface area;
DFT — density functional theory;
DOS — density of states;
DPA— diphenylacetylene;
ELF — electron localization function;
EXAFS — extended X-ray absorption fine structure;
FCC — face-centered cubic lattice;
HOPG — highly oriented pyrolytic graphite;
IMC — intermetallic compound;
LEED — low-energy electron diffraction;
LEIS — low energy ion scattering (spectroscopy);
PM-IRAS — polarization modulation infrared reflection-absorption spectroscopy;
SAA — single-atom alloy;
SR XPS — synchrotron radiation X-ray photoelectron spectroscopy;
STM — scanning tunnelling microscopy;
TEM — transmission electron microscopy;
TPD — temperature-programmed desorption;
UHV — ultra-high vacuum;
UPS — ultraviolet photoelectron spectroscopy;
XANES — X-ray absorption near-edge structure;
XPS — X-ray photoelectron spectroscopy.

6. References

1. A.Wang, X.Y.Liu, C.-Y.Mou, T.Zhang. *J. Catal.*, **308**, 258 (2013); https://doi.org/10.1016/j.jcat.2013.08.023
2. V.I.Bukhtiyarov, M.G.Slin'ko. *Russ. Chem. Rev.*, **70**, 147 (2001); https://doi.org/10.1070/RC2001v070n02ABEH000637
3. F.Tao, S.Zhang, L.Nguyen, X.Zhang. *Chem. Soc. Rev.*, **41**, 7980 (2012); https://doi.org/10.1039/c2cs35185d
4. F.Tao, M.E.Grass, Y.Zhang, D.R.Butcher, J.R.Renzas, Z.Liu, J.Y.Chung, B.S.Mun, M.Salmeron, G.A.Somorjai. *Science*, **322**, 932 (2008); https://doi.org/10.1126/science.1164170
5. F.Gao, D.W.Goodman. *Chem. Soc. Rev.*, **41**, 8009 (2012); https://doi.org/10.1039/c2cs35160a.
6. O.G.Ellert, M.V.Tsodikov, S.A.Nikolaev, V.M.Novotortsev. *Russ. Chem. Rev.*, **83**, 718 (2014); https://doi.org/10.1070/RC2014v083n08ABEH004432
7. M.Gholinejad, F.Khosravi, M.Afrasi, J.M.Sansano, C.Nájera. *Catal. Sci. Technol.*, **11**, 2652 (2021); https://doi.org/10.1039/D0CY02339F
8. J.E.S.van der Hoeven, J.Jelic, L.A.Olthof, G.Totarella, R.J.A.van Dijk-Moes, J.-M.Krafft, C.Louis, F.Studt, A.van Blaaderen, P.E.de Jongh. *Nat. Mater.*, **20**, 1216 (2021); https://doi.org/10.1038/s41563-021-00996-3
9. L.Liu, A.Corma. *Chem. Rev.*, **123**, 4855 (2023); https://doi.org/10.1021/acs.chemrev.2c00733.
10. S.A.Ten, M.D.Kurmanova, K.Kurmanbayeva, V.V.Torbina, O.A.Stonkus, O.V.Vodyankina. *Appl. Catal. A: General*, **674**, 119603 (2024); https://doi.org/10.1016/j.apcata.2024.119603
11. E.Ehret, E.Beyou, G.V.Mamontov, T.A.Bugrova, S.Prakash, M.Aouine, B.Domenichinid, F.J.Cadete Santos Aires. *Nanoscale*, **7**, 13239 (2015); https://doi.org/10.1039/C5NR02215K
12. M.S.Chen, D.Kumar, C.-W.Yi, D.W.Goodman. *Science*, **310**, 291 (2005); https://doi.org/10.1126/science.1115800
13. J.Xu, T.White, P.Li, C.H.He, J.G.Yu, W.K.Yuan, Y.F.Han. *J. Am. Chem. Soc.*, **132**, 10398 (2010); https://doi.org/10.1021/ja102617r
14. F.Gao, Y.L.Wang, D.W.Goodman. *J. Am. Chem. Soc.*, **131**, 5734 (2009); https://doi.org/10.1021/ja9008437
15. A.Sandoval, C.Louis, R.Zanella. *Appl. Catal. B: Environ.*, **140–141**, 363 (2013); https://doi.org/10.1016/j.apcatb.2013.04.039
16. F.Gao, Y.Wang, D.W.Goodman. *J. Catal.*, **268**, 115 (2009); https://doi.org/10.1016/j.jcat.2009.09.009
17. J.H.Song, D.Ch. Park, Y.-W.You, T.S.Chang, I.Heo, D.H.Kim. *Catal. Sci. Technol.*, **10**, 2120 (2020); https://doi.org/10.1039/C9CY02289A
18. J.K.Edwards, S.J.Freakley, A.F.Carley, Ch.J.Kiely, G.J.Hutchings. *Acc. Chem. Res.*, **47**, 845 (2014); https://doi.org/10.1021/ar400177c
19. Y.Zhang, W.Diao, C.T.Williams, J.R.Monnier. *Appl. Catal A: General*, **469**, 419 (2014); https://doi.org/10.1016/j.apcata.2013.10.024
20. A.J.McCue, J.A.Anderson. *Front. Chem. Sci. Eng.*, **9**, 142 (2015); https://doi.org/10.1007/s11705-015-1516-4
21. Y.Kotolevich, E.Pakrieva, E.Kolobova, M.H.Farías, N.Bogdanchikova, V.C.Corberán, D.Pichugina, N.Nikitina, S.A.C.Carabineiro, A.Pestryakov. *Catalysts*, **11**, 799 (2021); https://doi.org/10.3390/catal11070799
22. K.Qian, L.Luo, Z.Jiang, W.Huang. *Catal. Today*, **280**, 253 (2017); https://doi.org/10.1016/j.cattod.2016.03.035
23. F.Gao, Y.Wang, D.W.Goodman. *J. Phys. Chem. C*, **113**, 14993 (2009); https://doi.org/10.1021/jp9053132
24. X.Zhu, Q.Guo, Y.Sun, S.Chen, J.Q.Wang, M.Wu, W.Fu, Y.Tang, X.Duan, D.Chen, Y.Wan. *Nat. Commun.*, **10**, 1428 (2019); https://doi.org/10.1038/s41467-019-09421-5
25. J.K.Nørskov, T.Bligaard, J.Rossmeisl. *Nat. Chem.*, **1**, 37 (2009); https://doi.org/10.1038/nchem.121
26. A.Groß. *Top. Catal*. **37**, 29 (2006); https://doi.org/10.1007/s11244-006-0005-x
27. S.Zou, L.Wang, H.Wang, X.Zhang, H.Sun, X.Liao, J.Huang, A.R.Masri. *Energy Environ. Sci.*, **16**, 5513 (2023); https://doi.org/10.1039/D3EE01650A
28. Zh.-X.Chen, K.M.Neyman, N.Rösch. *Surf. Sci.*, **548**, 291 (2004); https://doi.org/10.1016/j.susc.2003.11.018
29. A.V.Bukhtiyarov, I.P.Prosvirin, A.A.Saraev, A.Yu.Klyushin, A.Knop-Gericke, V.I.Bukhtiyarov. *Faraday Discuss.*, **208**, 255 (2018); https://doi.org/10.1039/C7FD00219J
30. M.Mamatkulov, I.V.Yudanov, A.V.Bukhtiyarov, I.P.Prosvirin, V.I.Bukhtiyarov, K.M.Neyman. *J. Phys. Chem. C*, **123**, 8037 (2019); https://doi.org/10.1021/acs.jpcc.8b07402

31. L.Delannoy, S.Giorgio, J.G.Mattei, C.R.Henry, N.E.Kolli, C.Methivier, C.Louis. *ChemCatChem.*, **5**, 2707 (2013); https://doi.org/10.1002/cctc.201200618
32. B.Zugic, L.Wang, C.Heine, D.N.Zakharov, B.A.J.Lechner, E.A.Stach, J.Biener, M.Salmeron, R.J.Madix, C.M.Friend. *Nat. Mater.*, 16, 558 (2017); https://doi.org/10.1038/nmat4824
33. A.Wolfbeisser, G.Kovács, S.M.Kozlov, K.Föttinger, J.Bernardi, B.Klötzer, K.M.Neyman, G.Rupprechter. *Catal. Today*, **283**, 134 (2017); https://doi.org/10.1016/j.cattod.2016.04.022
34. E.Christoffersen, P.Stoltze, J.K.Nørskov. *Surf. Sci.*, **505**, 200 (2002); https://doi.org/10.1016/S0039-6028(02)01158-5
35. S.Zafeiratos, S.Piccinin, D.Teschner. *Catal. Sci. Technol.*, **2**, 1787 (2012); https://doi.org/10.1039/c2cy00487a
36. K.J.J.Mayrhofer, V.Juhart, K.Hartl, M.Hanzlik, M.Arenz. *Angew. Chem., Int. Ed.*, 48, 3529 (2009); https://doi.org/10.1002/anie.200806209
37. A.J.McCue, J.A.Anderson. *J. Catal.*, **329**, 538 (2015); https://doi.org/10.1016/j.jcat.2015.06.002
38. A.J.McCue, A.Gibson, J.A.Anderson. *Chem. Eng. J.*, **285**, 384 (2016); https://doi.org/10.1016/j.cej.2015.09.118
39. I.S.Mashkovsky, P.V.Markov, A.V.Rassolov, E.D.Patil, A.Yu.Stakheev. *Russ. Chem. Rev.*, **92** (8), RCR5087 (2023); https://doi.org/10.59761/RCR5087
40. L.Zhang, A.Wang, J.T.Miller, X.Liu, X.Yang, W.Wang, L.Li, Y.Huang, C.-Y.Mou, T.Zhang. *ACS Catal.*, **4**, 1546 (2014); https://doi.org/10.1021/cs500071c
41. G.X.Pei, X.Y.Liu, A.Wang, A.F.Lee, M.A.Isaacs, L.Li, X.Pan, X.Yang, X.Wang, Z.Tai, K.Wilson, T.Zhang. *ACS Catal.*, **5**, 3717 (2015); https://doi.org/10.1021/acscatal.5b00700
42. A.Yu.Fedorov, A.V.Bukhtiyarov, M.A.Panafidin, I.P.Prosvirin, I.A.Chetyrin, N.S.Smirnova, P.V.Markov, Y.V.Zubavichus, A.Yu.Stakheev, V.I.Bukhtiyarov. *Nano-Struct. Nano-Obj.*, **29**, 100830 (2022); https://doi.org/10.1016/j.nanoso.2021.100830
43. M.Wencka, M.Hahne, A.Kocjan, S.Vrtnik, P.Koželj, D.Korže, Z.Jagličić, M.Sorić, P.Popčević, J.Ivkov, A.Smontara, P.Gille, S.Jurga, P.Tomeš, S.Paschen, A.Ormeci, M.Armbrüster, Y.Grin, J.Dolinšek. *Intermetallics*, **55**, 56 (2014); https://doi.org/10.1016/j.intermet.2014.07.007
44. K.Kovnir, J.Osswald, M.Armbrüster, D.Teschner, G.Weinberg, U.Wild, A.Knop-Gericke, T.Ressler, Y.Grin, R.Schlögl. *J. Catal.*, **264**, 93 (2009); https://doi.org/10.1016/j.jcat.2009.03.007
45. A.Dasgupta, R.M.Rioux. *Catal. Today*, **330**, 2 (2019); https://doi.org/10.1016/j.cattod.2018.05.048
46. V.S.Marakatti, S.C.Peter. *Prog. Sol. State Chem.*, **52**, 1 (2018); https://doi.org/10.1016/j.progsolidstchem.2018.09.001
47. W.E.Wallace. *Annu. Rev. Phys. Chem.*, **15**, 109 (1964); https://doi.org/10.1146/annurev.pc.15.100164.000545
48. G.Bruni. *Chem. Rev.*, **1**, 345 (1925); https://doi.org/10.1021/cr60004a002
49. J.Wu, S.Shan, J.Luo, P.Joseph, V.Petkov, C.J.Zhong. *ACS Appl. Mater. Interf.*, **7**, 25906 (2015); https://doi.org/10.1021/acsami.5b08478
50. M.V.Castegnaro, A.Gorgeski, B.Balke, M.C.Alves, J.Morais. *Nanoscale*, **8**, 641 (2016); https://doi.org/10.1039/C5NR06685A
51. K.Kovnir, M.Armbrüster, D.Teschner, T.V.Venkov, F.C.Jentoft, A.Knop-Gericke, Y.Grin, R.Schlögl. *Sci. Technol. Adv. Mater.*, **8**, 420 (2007); https://doi.org/10.1016/j.stam.2007.05.004
52. C.Wang, D.P.Chen, X.Sang, R.R.Unocic, S.E.Skrabalak. *ACS Nano*, **10**, 6345 (2016); https://doi.org/10.1021/acsnano.6b02669
53. V.S.Marakatti, S.C.Sarma, B.Joseph, D.Banerjee, S.C.Peter. *ACS Appl. Mater. Interf.*, **9**, 3602 (2017); https://doi.org/10.1021/acsami.6b12253
54. R.Nesper. *Angew. Chem., Int. Ed.*, **30**, 789 (1991); https://doi.org/10.1002/anie.199107891
55. U.Mizutani. *Hume-rothery Rules for Structurally Complex Alloy Phases*. (CRC Press, 2016)
56. Z.Peng, H.You, H.Yang. *ACS Nano.*, **4**, 1501 (2010); https://doi.org/10.1021/nn9016795
57. M.Armbrüster. *Intermetallic Compounds in Catalysis. Encyclopedia of Catalysis*. (Wiley, 2002)
58. O.Deutschmann, H.Knözinger, K.Kochloefl, T.H.Turek. *Ullmann's Encyclopedia of Industrial Chemistry*. (Wiley-VCH, 2000)
59. R.Toyoshima, N.Hiramatsu, M.Yoshida, K.Amemiya, K.Mase, B.S.Mun, H.Kondoh. *J. Phys. Chem. C*, **120**, 416 (2016); https://doi.org/10.1021/acs.jpcc.5b10661
60. M.A.Languille, E.Ehret, H.C.Lee, C.K.Jeong, R.Toyoshima, H.Kondoh, K.Mase, Y.Jugnet, J.C.Bertolini, F.J.C.S.Aires, B.S.Mun. *Catal. Today*, **260**, 39 (2016); https://doi.org/10.1016/j.cattod.2015.05.029
61. H.Y.Kim, G.Henkelman. *ACS Catal.*, **3**, 2541 (2013); https://doi.org/10.1021/cs4006259
62. V.Soto-Verdugo, H.Metiu. *Surf. Sci.*, **601**, 5332 (2007); https://doi.org/10.1016/j.susc.2007.08.022
63. M.Ouyang, K.G.Papanikolaou, A.Boubnov, A.S.Hoffman, G.Giannakakis, S.R.Bare, M.Stamatakis, M.Flytzani-Stephanopoulos, E.Ch.H.Sykes. *Nat. Commun.*, **12**, 1549 (2021); https://doi.org/10.1038/s41467-021-21555-z
64. K.G.Papanikolaou, M.T.Darby, M.Stamatakis. *ACS Catal.*, **10**, 1224 (2020); https://doi.org/10.1021/acscatal.9b04029
65. K.G.Papanikolaou, M.T.Darby, M.Stamatakis. *J. Phys. Chem. C*, **123**, 9128 (2019); https://doi.org/10.1021/acs.jpcc.9b00649
66. A.V.Bukhtiyarov, I.P.Prosvirin, V.I.Bukhtiyarov. *Appl. Surf. Sci.*, **367**, 214 (2016); https://doi.org/10.1016/j.apsusc.2016.01.173
67. A.V.Bukhtiyarov, I.P.Prosvirin, M.A.Panafidin, A.Y.Fedorov, A.Y.Klyushin, A.Knop-Gericke, Y.V.Zubavichus, V.I.Bukhtiyarov. *Nanomaterials*, **11**, 3292 (2021); https://doi.org/10.3390/nano11123292
68. M.A.Panafidin, A.V.Bukhtiyarov, I.P.Prosvirin, Y.V.Zubavichus, V.I.Bukhtiyarov. *Surf. Interf.*, **41**, 103255:1 (2023); https://doi.org/10.1016/j.surfin.2023.103255
69. G.Sitja, C.R.Henry. *J. Phys. Chem. C*, **123**, 7961 (2019); https://doi.org/10.1021/acs.jpcc.8b07350
70. A.M.Venezia, L.F.Liotta, G.Deganello, Z.Schay, D.Horváth, L.Guczi. *Appl. Catal. A: General*, **211**, 167 (2001); https://doi.org/10.1016/S0926-860X(00)00870-X
71. V.R.Fernandes, M.Van Den Bossche, J.Knudsen, M.H.Farstad, J.Gustafson, H.J.Venvik, H.Grönbeck, A.Borg. *ACS Catal.*, **6**, 4154 (2016); https://doi.org/10.1021/acscatal.6b00658
72. M.D.Strømsheim, I.-H.Svenum, M.Mahmoodinia, V.Boix, J.Knudsen, H.J.Venvik. *Catal. Today*, **384–386**, 265 (2022); https://doi.org/10.1016/j.cattod.2021.02.007
73. M.A.Van Spronsen, K.Daunmu, C.R.O'Connor, T.Egle, H.Kersell, J.Oliver-Meseguer, M.B.Salmeron, R.J.Madix, P.Sautet, C.M.Friend. *J. Phys. Chem. C*, **123**, 8312 (2019); https://doi.org/10.1021/acs.jpcc.8b08849
74. V.Mehar, A.Almithn, T.Egle, M.-H.Yu, C.R.O'Connor, M.Karatok, R.J.Madix, D.Hibbitts, J.F.Weaver. *ACS Catal.*, **10**, 13878 (2020); https://doi.org/10.1021/acscatal.0c03885
75. A.P.Farkas, T.Diemant, J.Bansmann, R.J.Behm. *ChemPhysChem.*, **13**, 3516 (2012); https://doi.org/10.1002/cphc.201200477
76. I.S.Bondarchuk, G.V.Mamontov. *Kinet. Catal.*, **56**, 379, (2015); https://doi.org/10.1134/S0023158415030027
77. M.Zhao, J.C.Brouwer, W.G.Sloof, A.J.Böttger. *Int. J. Hydr. Energy*, **45**, 21576 (2020); https://doi.org/10.1016/j.ijhydene.2020.05.268
78. A.A.B.Padama, R.A.B.Villaos, J.R.Albia, W.A.Diño, H.Nakanishi, H.Kasai. *J. Phys.: Condens. Matter*, **29**, 025005 (2017); https://doi.org/10.1088/0953-8984/29/2/025005
79. A.A.B.Padama, A.P.S.Cristobal, J.D.Ocon, W.A.Diño, H.Kasai. *J. Phys. Chem. C*, **121**, 17818 (2017); https://doi.org/10.1021/acs.jpcc.7b02794

80. S.M.Kozlov, G.Kovács, R.Ferrando, K.M.Neyman. *Chem. Sci.*, **6**, 3868 (2015); https://doi.org/10.1039/C4SC03321C
81. L.Pleth Nielsen, F.Besenbacher, I.Stensgaard, E.Laegsgaard, C.Engdahl, P.Stoltze, K.W.Jacobsen, J.K.Nørskov. *Phys. Rev. Lett.*, **71**, 754 (1993); https://doi.org/10.1103/PhysRevLett.71.754
82. T.Marten, O.Hellman, A.V.Ruban, W.Olovsson, C.Kramer, J.P.Godowski, L.Bech, Z.Li, J.Onsgaard, I.A.Abrikosov. *Phys. Rev. B*, **77**, 125406 (2008); https://doi.org/10.1103/PhysRevB.77.125406
83. P.T.Wouda, M.Schmid, B.E.Nieuwenhuys, P.Varga. *Surf. Sci.*, **417**, 292 (1998); https://doi.org/10.1016/S0039-6028(98)00673-6
84. O.M.Løvvik. *Surf. Sci.*, **583**, 100 (2005); https://doi.org/10.1016/j.susc.2005.03.028
85. J.R.Kitchin, K.Reuter, M.Scheffler. *Phys. Rev. B*, **77**, 075437 (2008); https://doi.org/10.1103/PhysRevB.77.075437
86. B.C.Khanra, M.Menon. *Physica B: Condens. Matter*, **291**, 368 (2000); https://doi.org/10.1016/S0921-4526(00)00450-6
87. M.Ropo, K.Kokko, L.Vitos, J.Kollár. *Phys. Rev. B*, **71**, 045411 (2005); https://doi.org/10.1103/PhysRevB.71.045411
88. D.H.Kim, H.Y.Kim, H.G.Kim, J.H.Ryu, H.M.Lee. *J. Phys., Condens. Matter*, **20**, 035208 (2008); https://doi.org/10.1088/0953-8984/20/03/035208
89. S.González, K.M.Neyman, S.Shaikhutdinov, H.-J.Freund, F.Illas. *J. Phys. Chem. C*, **111**, 6852 (2007); https://doi.org/10.1021/jp071584v
90. H.L.Skriver, N.M.Rosengaard. *Phys. Rev. B*, **46**, 7157 (1992); https://doi.org/10.1103/PhysRevB.46.7157
91. M.Methfessel, D.Hennig, M.Scheffler. *Phys. Rev. B*, **46**, 4816 (1992); https://doi.org/10.1103/PhysRevB.46.4816.
92. J.P.Chan, R.Hultgren. *J. Chem. Therm.*, **1**, 45 (1969); https://doi.org/10.1016/0021-9614(69)90035-4
93. N.Eom, M.E.Messing, J.Johansson, K.Deppert. *ACS Nano.*, **15**, 8883 (2021); https://doi.org/10.1021/acsnano.1c01500
94. E.Christoffersen, P.Stoltze, J.K.Nørskov. *Surf. Sci.*, **505**, 200 (2002); https://doi.org/10.1016/S0039-6028(02)01158-5
95. I.-H.Svenum, J.A.Herron, M.Mavrikakis, H.J.Venvik. *Catal. Today*, **193**, 111 (2012); https://doi.org/10.1016/j.cattod.2012.01.007
96. G.Wowsnick, D.Teschner, I.Kasatkin, F.Girgsdies, M.Armbrüster, A.Zhang, Y.Grin, R.Schlögl, M.Behrens. *J. Catal.*, **309**, 209 (2014); https://doi.org/10.1016/j.jcat.2013.09.019
97. Z.Wu, E.C.Wegener, H.T.Tseng, J.R.Gallagher, J.W.Harris, R.E.Diaz, Y.Ren, F.H.Ribeiro, J.T.Miller. *Catal. Sci. Technol.*, **6**, 6965 (2016); https://doi.org/10.1039/C6CY00491A
98. M.Armbrüster, R.Schlögl, Y.Grin. *Sci. Technol. Adv. Mater.*, **15**, 034803 (2014); https://doi.org/10.1088/1468-6996/15/3/034803
99. D.Rosenthal, R.Widmer, R.Wagner, P.Gille, M.Armbrüster, Y.Grin, R.Schlögl, O.Gröning. *Langmuir*, **28**, 6848 (2012); https://doi.org/10.1021/la2050509
100. M.Kauppinen, H.Grönbeck. *Top. Catal.*, **66**, 1457 (2023); https://doi.org/10.1007/s11244-022-01748-6
101. S.A.Villaseca, A.Ormeci, S.V.Levchenko, R.Schlögl, Y.Grin, M.Armbrüster. *Chem. Phys. Chem.*, **18**, 334 (2017); https://doi.org/10.1002/cphc.201601162
102. A.V.Bukhtiyarov, M.A.Panafidin, I.A.Chetyrin, I.P.Prosvirin, I.S.Mashkovsky, N.S.Smirnova, P.V.Markov, Y.V.Zubavichus, A.Y.Stakheev, V.I.Bukhtiyarov. *Appl. Surf. Sci.*, **525**, 146493 (2020); https://doi.org/10.1016/j.apsusc.2020.146493
103. Q.Li, L.Song, L.Pan, Y.Chen, M.Ling, X.Zhuang, X.Zhang. *Appl. Surf. Sci.*, **288**, 69 (2014); https://doi.org/10.1016/j.apsusc.2013.09.116
104. N.S.Smirnova, I.S.Mashkovsky, P.V.Markov, A.V.Bukhtiyarov, G.N.Baeva, H.Falsig, A.Y.Stakheev. *Catalysts*, **11**, 1376 (2021); https://doi.org/10.3390/catal11111376
105. M.Schmid, R.J.Madix, C.M.Friend. *Surf. Sci.*, **643**, 36 (2016); https://doi.org/10.1016/j.susc.2015.08.023
106. K.Tang, T.Wang, W.Qi, Y.Li. *Physica B: Condens. Matter*, **531**, 95 (2018); https://doi.org/10.1016/j.physb.2017.12.025
107. M.Friedrich, A.Ormeci, Y.Grin, M.Armbrüster. *Z. Anorg. Allg. Chem.*, **636**, 1735 (2010); https://doi.org/10.1002/zaac.201000097
108. H.Guesmi, C.Louis, L.Delannoy. *Chem. Phys. Lett.*, **503**, 97 (2011); https://doi.org/10.1016/j.cplett.2010.12.064
109. O.V.Vinogradova, K.Reuter, V.J.Bukas. *J. Phys. Chem. C*, **127**, 22060 (2023); https://doi.org/10.1021/acs.jpcc.3c05640
110. J.R.Kitchin, K.Reuter, M.Scheffler. *Phys. Rev. B*, **77**, 075437 (2008); https://doi.org/10.1103/PhysRevB.77.075437
111. N.Golio, A.J.Gellman. *ACS Catal.*, **13**, 14548 (2023); https://doi.org/10.1021/acscatal.3c03253
112. É.Gaudry, G.M.McGuirk, J.Ledieu, V.Fournée. *J. Chem. Phys.*, **141**, 084703 (2014); https://doi.org/10.1063/1.4892409
113. S.Furukawa, T.Komatsu. *ACS Catal.*, **7**, 735 (2017); https://doi.org/10.1021/acscatal.6b02603
114. J.Osswald, R.Giedigkeit, R.E.Jentoft, M.Armbrüster, F.Girgsdies, K.Kovnir, T.Ressler, Y.Grin, R.Schlögl. *J. Catal.*, **258**, 210 (2008); https://doi.org/10.1016/j.jcat.2008.06.013
115. J.Osswald, K.Kovnir, M.Armbrüster, R.Giedigkeit, R.E.Jentoft, U.Wild, Yu.Grin, R.Schlögl. *J. Catal.*, **258**, 219 (2008); https://doi.org/10.1016/j.jcat.2008.06.014
116. M.Armbrüster, K.Kovnir, M.Behrens, D.Teschner, Yu.Grin, R.Schlögl. *J. Am. Chem. Soc.*, **132**, 14745 (2010); https://doi.org/10.1021/ja106568t
117. G.Wowsnick, D.Teschner, M.Armbrüster, I.Kasatkin, F.Girgsdies, Yu.Grin, R.Schlögl, M.Behrens. *J. Catal.*, **309**, 211 (2014); https://doi.org/10.1016/j.jcat.2013.09.018
118. P.V.Markov, A.V.Bukhtiyarov, I.S.Mashkovskii, N.S.Smirnova, I.P.Prosvirin, Z.S.Vinokurov, M.A.Panafidin, G.N.Baeva, Y.V.Zubavichus, V.I.Bukhtiyarov, A.Y.Stakheev. *Kinet. Catal.*, **60**, 842 (2019); https://doi.org/10.1134/S0023158419060065
119. D.B.Burueva, K.V.Kovtunov, A.V.Bukhtiyarov, D.A.Barskiy, I.P.Prosvirin, I.S.Mashkovsky, G.N.Baeva, V.I.Bukhtiyarov, A.Y.Stakheev, I.V.Koptyug. *Chem. – Eur. J.*, **24**, 2547 (2018); https://doi.org/10.1002/chem.201705644
120. S.Guo, K.Heck, S.Kasiraju, H.Qian, Z.Zhao, L.C.Grabow, J.T.Miller, M.S.Wong. *ACS Catal.*, **8**, 503 (2018); https://doi.org/10.1021/acscatal.7b01371
121. Y.Men, G.Kolb, R.Zapf, M.O'Connell, A.Ziogas. *Appl. Catal. A: General*, **380**, 15 (2010); https://doi.org/10.1016/j.apcata.2010.03.004
122. A.García-Trenco, A.Regoutz, E.R.White, D.J.Payne, M.S.P.Shaffer, C.K.Williams. *Appl. Catal. B: Environ.*, **220**, 9 (2018); https://doi.org/10.1016/j.apcatb.2017.07.069
123. P.Wu, B.Yang. *Catal. Sci. Technol.*, **9**, 6102 (2019); https://doi.org/10.1039/C9CY01242G
124. M.A.Panafidin, A.V.Bukhtiyarov, I.P.Prosvirin, I.A.Chetyrin, A.Y.Klyushin, A.Knop-Gericke, N.S.Smirnova, P.V.Markov, I.S.Mashkovsky, Y.V.Zubavichus, A.Y.Stakheev, V.I.Bukhtiyarov. *Appl. Surf. Sci.*, **571**, 151350 (2022); https://doi.org/10.1016/j.apsusc.2021.151350
125. N.S.Smirnova, E.V.Khramov, G.N.Baeva, P.V.Markov, A.V.Bukhtiyarov, Y.V.Zubavichus, A.Y.Stakheev. *Catalysts.*, **11**, 859 (2021); https://doi.org/10.3390/catal11070859
126. L.Meng, X.Han, L.Yu, Y.Wang. *J. Environ. Sci.*, **124**, 371 (2023); https://doi.org/10.1016/j.jes.2021.08.051
127. S.Shetty, M.Gayen, S.Agarwal, D.Chatterjee, A.Singh, N.Ravishankar. *J. Phys. Chem. Lett.*, **13**, 770 (2022); https://doi.org/10.1021/acs.jpclett.1c03852
128. N.S.Smirnova, P.V.Markov, G.N.Baeva, A.V.Rassolov, I.S.Mashkovsky, A.V.Bukhtiyarov, I.P.Prosvirin, M.A.Panafidin, Y.V.Zubavichus, V.I.Bukhtiyarov, A.Y.Stakheev. *Mendeleev Commun.*, **29**, 547 (2019); https://doi.org/10.1016/j.mencom.2019.09.023
129. A.V.Bukhtiyarov, M.A.Panafidin, I.P.Prosvirin, I.S.Mashkovsky, P.V.Markov, A.V.Rassolov, N.S.Smirnova, G.N.Baeva, C.Rameshan, R.Rameshan, Y.V.Zubavichus, V.I.Bukhtiyarov, A.Yu.Stakheev. *Appl. Surf. Sci.*, **604**, 154497 (2022); https://doi.org/10.1016/j.apsusc.2022.154497

130. I.S.Mashkovsky, N.S.Smirnova, P.V.Markov, G.N.Baeva, G.O.Bragina, A.V.Bukhtiyarov, I.P.Prosvirin, A.Y.Stakheev. *Mendeleev Commun.*, **28**, 603 (2018); https://doi.org/10.1016/j.mencom.2018.11.013
131. A.V.Bukhtiyarov, M.A.Panafidin, I.P.Prosvirin, N.S.Smirnova, P.V.Markov, G.N.Baeva, I.S.Mashkovsky, G.O.Bragina, C.Rameshan, E.Y.Gerasimov, Y.V.Zubavichus, V.I.Bukhtiyarov, A.Y.Stakheev. *Appl. Surf. Sci.*, **608**, 155086 (2023); https://doi.org/10.1016/j.apsusc.2022.155086
132. N.Marcella, J.S.Lim, A.M.Płonka, G.Yan, C.J.Owen, J.E.S.van der Hoeven, A.C.Foucher, H.T.Ngan, S.B.Torrisi, N.S.Marinkovic, E.A.Stach, J.F.Weaver, J.Aizenberg, Ph.Sautet, B.Kozinsky, A.I.Frenkel. *Nat. Commun.*, **13**, 832 (2022); https://doi.org/10.1038/s41467-022-28366-w
133. J.D.Lee, J.B.Miller, A.V.Shneidman, L.Sun, J.F.Weaver, J.Aizenberg, J.Biener, J.A.Boscoboinik, A.C.Foucher, A.I.Frenkel, J.E.S.van der Hoeven, B.Kozinsky, N.Marcella, M.M.Montemore, H.T.Ngan, Ch.R.O'Connor, C.J.Owen, D.J.Stacchiola, E.A.Stach, R.J.Madix, Ph.Sautet, C.M.Friend. *Chem. Rev.*, **122**, 8758 (2022); https://doi.org/10.1021/acs.chemrev.1c00967
134. K.G.Papanikolaou, M.T.Darby, M.Stamatakis. *ACS Catal.*, **10**, 1224 (2020); https://doi.org/10.1021/acscatal.9b04029
135. H.Li, W.Chai, G.Henkelman. *J. Mater. Chem. A*, **7**, 23868 (2019); https://doi.org/10.1039/C9TA04572D
136. A.Filie, T.Shirman, A.C.Foucher, E.A.Stach, M.Aizenberg, J.Aizenberg, C.M.Friend, R.J.Madix. *J. Catal.*, **404**, 943 (2021); https://doi.org/10.1016/j.jcat.2021.06.003
137. P.V.Markov, N.S.Smirnova, G.N.Baeva, I.S.Mashkovsky, A.V.Bukhtiyarov, I.A.Chetyrin, Y.V.Zubavichus, A.Yu.Stakheev. *Mendeleev Commun.*, **33**, 812 (2023); https://doi.org/10.1016/j.mencom.2023.10.024
138. A.V.Bukhtiyarov, M.A.Panafidin, I.P.Prosvirin, N.S.Smirnova, P.V.Markov, G.N.Baeva, I.S.Mashkovsky, G.O.Bragina, Z.S.Vinokurov, Y.V.Zubavichus, V.I.Bukhtiyarov, A.Yu.Stakheev. *Crystals*, **13**, 1356 (2023); https://doi.org/10.3390/cryst13091356